Bioamplification as a Bioaccumulation Mechanism for Persistent Organic Pollutants (POPs) in Wildlife

Jennifer M. Daley, Gordon Paterson, and Ken G. Drouillard

Contents

1 Introduction

Bioaccumulation describes the process by which anthropogenic chemicals are taken up by organisms from their environment and diet and are subsequently assimilated and distributed into tissues (Arnot and Gobas 2003; Borgå et al. 2004; Mackay and Fraser 2000). Thus, bioaccumulation is a central framework within ecotoxicology, because it

J.M. Daley (✉) • G. Paterson • K.G. Drouillard
Great Lakes Institute for Environmental Research, University of Windsor,
Windsor, ON, Canada N9B 3P4
e-mail: daleyj@uwindsor.ca

D.M. Whitacre (ed.), *Reviews of Environmental Contamination and Toxicology Volume 227*, Reviews of Environmental Contamination and Toxicology 227,
DOI 10.1007/978-3-319-01327-5_4,

helps define the maximum concentration that can be achieved by an organism in its tissues, relative to the exposure media, and helps determine the potential chemical dose/toxicity experienced by an individual. Therefore, understanding the dynamic processes that regulate chemical bioaccumulation in animals is essential for protecting species, ecosystems, and ultimately human health (Arnot and Gobas 2004; Kelly et al. 2004).

The rationale for studying the bioaccumulation of persistent organic pollutants (POPs) derives mainly from the high potential some organisms (and associated food webs) have to bioaccumulate them. Several reviews have been published on the bioaccumulation of POPs in biota, and the approaches used to model their bioaccumulation (Barber 2003, 2008; Connell 1988; Gobas 1993a; Gobas and Morrison 2000; Mackay and Fraser 2000; Nichols et al. 2009; Selck et al. 2012; Thomann 1981; Thomann et al. 1992; Walker 1990). State of the art POP bioaccumulation models continue to evolve and now incorporate many diverse concepts. These concepts include: hydrophobicity-driven equilibrium partitioning (DeBruyn and Gobas 2007; Gobas et al. 1986; Hamelink et al. 1971; Mackay 1982, Neely et al. 1974; Veith et al. 1979), bioavailability constraints related to chemical sequestration in abiotic organic and inorganic carbon matrices (Black and McCarthy 1988; Cornelissen et al. 2005; Lohmann et al. 2005), biomagnification related to chemical exposure from food, and complex food web feeding relationships (Alonso et al. 2008; Arnot and Gobas 2004; Borgå et al. 2012; Campfens and Mackay 1997; Gobas et al. 1993b; Morrison et al. 1997; Thomann et al. 1992), and biological vectors as sources of POPs introduction to and from ecosystems (Ewald et al. 1998; Gregory-Eaves et al. 2007; Krummel et al. 2003). More recently, biological mechanisms across a given species' life cycle have also been described (Hickie et al. 1999, 2005, 2007; Ng and Gray 2009; Sijm et al. 1992; Yordy et al. 2010; Zhao et al. 2007).

The focus of this review is to draw attention to a non-steady state, non-equilibrium mechanism of bioaccumulation, herein described as bioamplification. In this paper, we apply bioamplification to POPs. The term bioamplification has recently been coined to define the condition in which an organism loses body weight and chemical partitioning capacity at a faster rate than it can eliminate those chemicals (Daley et al. 2009, 2011). This causes an increase in the chemical concentration in the organism and in its tissues, when concentrations are expressed on a wet weight basis. A much greater increase in the concentration of chemical occurs, when tissue residues are expressed on a lipid-normalized basis. Although the term bioamplification has been used previously in ecotoxicology to describe mercury biomagnification (Potter et al. 1975), and is sometimes used as the French translation of biomagnification, the past use of this term has been largely superseded by "biomagnification" (Connolly and Pedersen 1988). Notably, bioamplification is mechanistically distinguished from other bioaccumulation mechanisms (e.g., bioconcentration and biomagnification, see Sect. 2 below) in that concentrations of chemical become enriched in the organism without a change in the chemical mass balance in the animal, or when the concentration enrichment exceeds the mass increase of a chemical. MacDonald et al. (2002) explained this process as being analogous to solvent depletion and one of several mechanisms (e.g., biomagnification) that contributes to "amplification" of chemical residues in organism tissues. Although bioamplification

is an independent bioaccumulation process that interacts with both bioconcentration and biomagnification processes, it is rarely acknowledged or specifically addressed in risk assessments or in the bioaccumulation modelling literature.

2 Bioamplification as an Independent Bioaccumulation Mechanism

The POPs literature has classically defined bioaccumulation as being contributed to by two main processes: bioconcentration and biomagnification. Both of these processes are individually defined by how chemical exposures to the animal occur (see below). The two processes are commonly distinguished from one another on the basis that bioconcentration is often modeled as an equilibrium partitioning process (Barber 2003; Mackay 1982), whereas biomagnification is modeled as a non-equilibrium kinetic process (Gobas et al. 1988). For clarity, the differences between bioconcentration, biomagnification, and bioamplification are defined and described below.

Bioconcentration describes the diffusive transport of chemicals across respiratory surfaces (Barber et al. 1988; Barber 2003; Leblanc 1995; Neely et al. 1974). Through bioconcentration, the organism accumulates and eventually equilibrates with its respired media via respiratory exchange and can approach or achieve a chemical fugacity similar to its respired media (Di Toro et al. 1991; Landrum et al. 2001). Chemical fugacity is defined by the criteria for establishing chemical equilibrium in reference to both the chemical concentration and partitioning capacity of the sample (Mackay 1979; Schwarzenbach et al. 1993). For biological samples, chemical fugacity (Pa) is calculated as the chemical concentration (C_{org}, mol/m^3) divided by the equilibrium distribution coefficient for the chemical of interest between the sample and air (Z_{org}, mol/m^3/Pa) (Mackay 1979; Mackay and Paterson 1981). When the chemical fugacity is equal between two interacting environmental media, the samples are considered to be in equilibrium with one another. This consideration of chemical equilibrium cannot be deduced by direct comparison of wet weight chemical concentrations. However, kinetic-based bioconcentration models can be used to describe the approach of chemical fugacity toward equilibrium in an organism relative to its respired media.

Equilibrium partitioning-based bioconcentration models have shown a high degree of success for predicting POP bioaccumulation in laboratory bioconcentration tests, when water is the predominant exposure route (Di Toro et al. 1991; Landrum et al. 2001; Mackay 1982; Meylen et al. 1999). Under field conditions, the equilibrium partitioning model appears to be best suited to negligibly biotransformed hydrophobic organic chemicals over a log K_{OW} range of approximately 3–5 (Barber 2008; Gobas and Morrison 2000; Meylen et al. 1999). Several comprehensive reviews of, and modelling approaches to bioconcentration have been completed (Arnot and Gobas 2006; Barber 2003; Barron 1990; Connell 1988; Devillers et al. 1998; Gobas and Morrison 2000; Mackay and Fraser 2000). Bioconcentration can be complicated when organisms respire water from both overlying and pore waters that are associated

with sediments (DiToro et al. 1991), and when these different water sources exhibit differences in chemical fugacity (DeBruyn and Gobas 2004). Furthermore, the bioconcentration process is complicated by the presence of constituents in water and sediments (viz., suspended solids, dissolved organic matter, and/or black carbon) that alter chemical bioavailability and the freely dissolved concentrations of chemical in the respired media (Black and McCarthy 1988; Cornelissen et al. 2005).

Biomagnification is a non-equilibrium bioaccumulation process, and is commonly modeled under steady state conditions (Drouillard 2008). Biomagnification occurs when chemical exposures occur via ingestion of contaminated food (Connolly and Pedersen 1988). For negligibly biotransformed, highly hydrophobic chemicals, biomagnification can result in the chemical fugacity of an animal exceeding that of its food (DeBruyn and Gobas 2006; Gobas et al. 1993b; Kelly et al. 2007a). This can translate into elevated chemical fugacities in the organism, compared to the respired environmental media (Connolly and Pedersen 1988; Morrison et al. 1997). The relative importance of bioconcentration and biomagnification to the uptake and overall chemical bioaccumulation potential varies and depends on several factors that include the following: chemical hydrophobicity, chemical elimination rates, differences in chemical fugacity between ingested food and respired media, and whether the chemical fugacity in the animal is well below, approaching, or exceeds the chemical fugacity in its respired media. The increased chemical fugacity in organisms resulting from contaminated food exposures can further propagate through successive trophic levels in a food web, and produce non-equilibrium food web biomagnification (Connolly and Pedersen 1988). Food web biomagnification of POP compounds has been widely demonstrated to occur for multiple animal species from both aquatic (Oliver and Niimi 1988; Russell et al. 1999a) and terrestrial (Czub and McLachlan 2004; Kelly and Gobas 2001, 2003; McLachlan 1996) food webs. A number of models have described the biomagnification of POPs in organisms and food webs (Arnot and Gobas 2004; Drouillard et al. 2012; Gobas et al. 1988, 1999; Kelly et al. 2004; Mackay and Fraser 2000; McLachlan 1996; Schlummer et al. 1998).

Both bioamplification and biomagnification can be empirically distinguished from bioconcentration as mechanisms that raise the chemical fugacity of the organism above that of its respired media and that of its food. Bioamplification is distinguished from biomagnification in that the chemical fugacity in an animal is increased without a change in the chemical uptake rate into the organism. This specifically occurs when the animal experiences a rapid decrease in the partitioning capacity of its tissues at a rate that exceeds the chemical elimination rate. The result is that the chemical fugacity of the organism experiences an increase, even though the total mass of chemical in the organism does not change, or, if it does change, it does so to a lesser extent than the fugacity change that was measured. Therefore, bioamplification occurs when there is a shift from steady state to non-steady state conditions as precipitated by a rapid weight loss event. Bioamplification may also occur during the uptake portion of the non-steady state bioaccumulation curve. In this case, bioamplification increases the chemical fugacity of the animal over what would be normal for a non-steady state uptake trajectory, if no change in partitioning capacity was experienced by the animal. Bioamplification is more difficult to distinguish during

the uptake phase of the non-steady state bioaccumulation process. Properly defining bioamplification under this scenario requires simultaneous determination of partitioning capacity changes, as well as characterizing changes in the mass balance of chemical in the animal. As in the steady state case above, bioamplification is verified when the change in chemical fugacity of the animal over a period of time exceeds the change in chemical mass balance in the animal over the same time interval.

A chief characteristic of bioamplification is that it results from weight loss. Negative growth in an organism and reduced partitioning capacity for the chemical under study are specific characteristics of bioamplification. Although growth dilution has long been adopted within bioaccumulation models, growth is commonly assumed to be constant and positive (Clark et al. 1990; Gobas 1993a). Notwithstanding, growth is known to be highly dynamic over an animal's life cycle, and is highly influenced by ecological and physiological factors (Blais et al. 2003; Chiuchiolo et al. 2004; Czub and McLachlan 2004; DeBruyn and Gobas 2006; Hickie et al. 1999; MacDonald et al. 2002; Ng and Gray 2009; Norstrom et al. 2007). Growth dilution (or biodilution) becomes a non-steady state process when the growth rate of an organism changes over a period of time that is shorter than the time required for the animal to re-achieve steady state with a chemical in its environment (McLachlan 1996). Although it has not been well studied, many animal species are known to lose weight during certain periods of their life histories. These weight loss events drive bioamplification, which represents the opposite of growth dilution (Clark et al. 1990; Kelly et al. 2004). Unless the animal dies, weight loss is predominantly a temporary condition, and is therefore often ignored or negated in bioaccumulation models. Therefore, bioamplification is not typically considered in steady state bioaccumulation models, because weight loss is not a component of the model algorithms. Arguably, excluding weight loss from bioaccumulation models has reduced interest in evaluating bioamplification as a separate phenomenon in natural systems (Gabrielsen et al. 1995; MacDonald et al. 2002).

Bioamplification, bioconcentration, and biomagnification are attenuated by chemical elimination. Chemical elimination restricts the types of chemicals and organisms for which bioamplification is likely to occur. Although bioamplification will always occur during weight loss events, the extent depends on the rate of chemical elimination and the loss of partitioning capacity. Bioamplification will be maximized for POPs in aquatic food webs that (1) exhibit high hydrophobicity, because hydrophobicity inversely correlates with chemical elimination (Kelly et al. 2007a; Paterson et al. 2007ab), and (2) for chemicals that undergo little or no metabolic biotransformation (Boon et al. 1989, 1994; Rasmussen et al. 1990; Safe 1994). Consequently, bioamplification will be most prominent for chemicals that have high log K_{OW} (>6.5) values, and exhibit food web biomagnification (Clark et al. 1990). For terrestrial food webs, chemicals that possess a log K_{OW} >2 and a log K_{OA} (octanol–air partition coefficient) >6 should be regarded as having a high bioamplification potential, because they display slow respiratory elimination (Drouillard et al. 2012; Kelly et al. 2007a). From the organismal perspective, bioamplification is expected to occur in those species that exhibit: (1) pronounced weight or lipid loss at specific times during their life cycles and (2) slow elimination kinetics of chemicals relative

to the time frame required to produce weight loss. In the latter case, the extent of bioamplification achieved by an individual is expected to be correlated with animal body size, inversely related to the metabolic biotransformation capacity of the animal and, in most cases, be greater for terrestrial than aquatic organisms (Drouillard and Norstrom 2000; Fisk et al. 1998; Kelly and Gobas 2001, 2003; Kelly et al. 2007a; Paterson et al. 2007b).

3 Measurement of Bioamplification

The manner in which bioamplification is characterized is similar to how chemical bioconcentration factors (BCF), bioaccumulation factors (BAF), and biomagnification factors (BMF) are quantified. In particular, the degree of bioamplification is characterized by expressing the ratio of chemical fugacity in an animal ($f_{\mathrm{org}(t)}$) relative to a reference state. Specifically, the reference state refers to the chemical fugacity of the animal prior to the weight loss event ($f_{\mathrm{org}(t-1)}$). Hence, the bioamplification factor (BAmF) in fugacity notation is defined as:

$$BAmF = \frac{f_{org(t)}}{f_{org(t-1)}} \tag{1}$$

Alternatively, bioamplification can be expressed as the ratio of lipid-normalized or lipid-equivalent chemical concentrations for the animal post versus pre-weight loss events (see below).

If the animal has achieved steady state with its environment prior to the initial sampling event, a BAmF >1 provides evidence that bioamplification has occurred. Bioamplification can be further confirmed if both the BAmF >1 and the mass balance of chemical in the animal has not changed. Under non-steady state uptake conditions, the BAmF will always exceed 1, even when bioamplification does not occur. Under these circumstances, bioamplification can only be distinguished from bioconcentration and biomagnification by factoring in both the chemical mass balance in the animal and the BAmF ratio. When the magnitude of the BAmF is >1 and also exceeds the change in chemical mass balance in the organism, both following and prior to weight loss, bioamplification can be regarded to have occurred. Finally, under conditions of net chemical elimination, which may occur after an animal switches to a less contaminated diet, BAmFs >1 are always indicative of bioamplification. Since the status of an organism (i.e., steady state, non-steady state net uptake, or non-steady state net depuration) is rarely known when samples are collected in the field, BAmFs should generally be interpreted in conjunction with the chemical mass balance determined in the animal over the same time interval.

BAmFs are best described as changes in chemical fugacity, but lipid-normalized and lipid-equivalent ratios may be used as surrogate measures for chemical fugacity. Differences in the partitioning capacity of animals and their respective tissues are commonly calculated on the basis of the lipid content of the sample (Mackay and

Paterson 1981). Thus, correcting or normalizing for lipid content standardizes the fugacity capacity of different biological sample types. This normalization permits the comparison of relative chemical fugacities between differing sample types (Clark et al. 1988, 1990; Mackay 1991). BAmFs, expressed as the ratio of lipid-normalized concentrations in an animal at two time intervals, are expressed as:

$$BAmF = \frac{C_{org(t)}}{C_{org(t-1)}} \times \frac{X_{lipid(t-1)}}{X_{lipid(t)}} \tag{2}$$

Where $C_{org(t)}$, $C_{org(t-1)}$ are the chemical concentrations (ng/g wet weight) in the animal at the two time intervals, and $X_{lipid(t)}$, and $X_{lipid(t-1)}$ refer to the mass fraction of lipid (g/g body weight) in the animal at each time interval, respectively.

Bioamplification is most often a direct consequence of lipid loss. Consequently, when studying this phenomenon it is important to accurately quantify lipids. However, it is important to note that the lipid content of tissue samples is usually operationally defined by the analytical method used to determine the lipids. Lipids are usually extracted from tissue samples with solvents that are then evaporated, and then subjected to gravimetric analysis (Drouillard et al. 2004; Randall et al. 1998). Since solvent combinations used to extract lipids vary among studies, it is important to maintain consistency of method for lipid analysis in any comparative study. However, some lipid determination methods provide better surrogate measures of partitioning capacity than others. For example, Randall et al. (1998) recommended that the Bligh and Dyer (1959) technique, which uses a chloroform–methanol solvent mixture for total lipid extraction, be used for lipid normalization, because this method co-extracts both polar and neutral lipids (McElroy et al. 2011). Drouillard et al. (2004) compared lipid extractions from chloroform–methanol and dichloromethane–hexane in fish tissues and found the two methods to produce different lipid results. However, when the authors compared lipid-normalized POP concentrations between tissues of individual fish, it was found that the dichloromethane–hexane procedure best compensated for differences in tissue partitioning capacities. Specifically, lipid-normalized POP concentrations between tissues were lower, when lipids from the dichloromethane–hexane extraction procedure were utilized. The authors concluded that solvent mixtures that extract neutral rather than total lipids are most appropriate when the lipid result is used to measure POP partitioning capacity of tissues. Unfortunately, lipid determination methods are rarely standardized across studies, and most typically utilize the same solvent combinations as for chemical extraction.

More recently, researchers have recognized that neutral lipids are not the only contributors to partitioning capacity of hydrophobic POPs in animal tissues. Biological sample partitioning capacities can be underestimated when the lipid content of the sample drops below 1% (DeBruyn and Gobas 2007; Gobas et al. 1999). Gobas et al. (1999) defined non-lipid organic matter (NLOM), essentially referring to lean dry protein (LDP) content, as having a partitioning capacity of approximately 3% of that provided by neutral lipids. DeBruyn and Gobas (2007) later revised this estimate to define the partitioning capacity of lean dry matter as having 5% of the partitioning capacity of neutral lipid. For organisms or tissue samples having low lipid content, the lipid-equivalent concentration is suggested to better

represent chemical fugacity than lipid normalized concentrations. However, obtaining estimates of NLOM or LDP requires analyzing both the neutral lipid content and moisture content of the sample. Expressing the BAmF on a lipid-equivalents basis is calculated as follows:

$$BAmF = \frac{C_{org(t)}}{C_{org(t-1)}} \times \frac{\left(X_{lipid(t-1)} + 0.05X_{LDP(t-1)}\right)}{\left(X_{lipid(t)} + 0.05X_{LDP(t)}\right)} \tag{3}$$

Where $X_{\mathrm{LDP}(t-1)}$ and $X_{\mathrm{LDP}(t)}$ refer to the mass fraction of lean dry protein in the sample at each time interval. Lean dry protein content (g) is typically calculated by subtracting the water content (g) and lipid content (g) from the wet weight (g) of the sample.

4 Bioamplification Case Studies

Animal energetics encompasses the processes through which individuals acquire, assimilate, and allocate their food resources (Humphries et al. 2004; McNab 2001). To compensate for metabolic demands that are imposed by periods of energy imbalances in an animal's life cycle, animals are frequently required to rely on accumulated somatic energy reserves. These periods, although perhaps brief, are expected to coincide with weight loss and bioamplification. In addition to generating water from catabolism, lipids are the most calorically rich tissue reserves, providing up to eight times the total energy available from protein and carbohydrate stores (McWilliams et al. 2004). Consequently, animals that maximize their lipid reserves prior to periods of nutritional stress are those most likely to successfully endure the event. The rates at which lipids are mobilized during a bioenergetic bottleneck depends on several key factors that include an animal's field metabolic rate as influenced by basal metabolism, thermoregulation costs and activity, and the duration of the bottleneck itself (Humphries et al. 2004). Although lipids are a critical component for surviving energetically demanding events, protein turnover is also required for muscle repair. Moreover, species that undergo periods of intense exercise (i.e., migrations) require large protein stores (Golet and Irons 1999). Body size also matters, because large-bodied individuals often better withstand prolonged starvation events from their higher ratio of somatic energy reserves to metabolic rate (Bystrom et al. 2006). Bioamplification of hydrophobic organic chemicals is predicted to occur frequently in nature, because mobilization of somatic lipid stores, and to a lesser extent, lean dry protein, represents the primary response of animals under conditions of an energy imbalance.

Fasting occurs in nearly all major taxonomic groups and often extends over prolonged periods (Wang et al. 2006). Many animal species inhabit highly variable environments where nutrient abundance and quality are inconsistent and periods of starvation are common (Kirk 1997). Winter is often the most significant and recurring period of energy imbalance experienced by animals during their life history. Nutrient abundance is a particular constraint for species inhabiting north temperate

or Arctic climatic zones, where cold temperature periods last several months and dominate the annual temperature cycle (Fort et al. 2009; Webster and Hartman 2007). Low temperatures, decreased food and water availability, and potential ice cover all exacerbate the energetic imbalances that animals experience during overwintering events. Animals often respond to suboptimal cold temperatures by employing specific strategies such as migration or hibernation, both of which entail bioenergetic consequences and can be associated with weight loss (Yahner 2012). Bioenergetic bottlenecks also result from natural physiological events that occur during the animals' life history. This includes events such as metamorphosis, molting, and reproduction (Golet et al. 2000; Lambert and Dutil 2000; Orlofske and Hopkins 2009). Although less common, weight loss may also result from disease.

In the following sections, we review bioamplification across taxonomic groups by examining laboratory and field studies that have been performed during different life stages or under different developmental conditions. These stages or conditions include embryo and larval development, metamorphosis, reproduction, overwintering, hibernation, migration and at other times of nutritional stress (e.g., disease). In Table 1, we present a list of selected cases studies from the literature that demonstrate bioamplification.

4.1 Bioamplification During Embryo and Juvenile Development

In addition to representing a highly dynamic period of tissue differentiation and animal development, embryo development for oviparous species is characterized by a dependence on maternally provided food resources. During this period, the mobilization of endogenous lipid and protein reserves by the developing embryo has the potential to generate conditions suitable for POPs bioamplification (Kleinow et al. 1999). Over the past 10 years, evidence for embryonically derived bioamplification has been observed among avian and fish species. For example, Drouillard et al. (2003) developed a bioenergetic model for herring gull (*Larus argentatus*) embryos during the egg incubation period that predicted a steady decline in egg lipid mass during incubation. During this life stage, lipid-normalized polychlorinated biphenyl (PCB) concentrations that were quantified in developing chicks increased as a function of incubation date (Drouillard et al. 2003). Significantly, for pipping chicks, lipid-normalized PCB concentrations were higher than those quantified in the egg laying females (Drouillard et al. 2003). However, following hatching and the initiation of exogenous feeding, growth dilution quickly attenuated the extent of bioamplification occurring in growing chicks (Drouillard et al. 2003).

For fish species such as yellow perch (*Perca flavescens*) and Chinook salmon (*Oncorhynchus tshawytscha*), life history characteristics can differ substantially during the embryo and larval development periods (Scott and Crossman 1973). Yellow perch spawn in the spring and are iteroparous (characterized by multiple reproductive events), wherein the larval stage emerges as free swimming individuals that are capable of external feeding (Post and McQueen 1988). In contrast,

Table 1 A list of case studies demonstrating bioamplification across taxonomic groups

Species	Life history	Sex	Field/experimental	Chemicals[a]	Tissues	$BAmF_{max}$	Reference
Invertebrates							
Mayflies (*Hexagenia* spp.)	Reproductive flight	M	Field	PCBs	Whole	3.4	(Daley et al. 2011)[b]
Amphibians							
Green frogs (*Rana clamitans*)	Metamorphosis	M/F	Experimental	PCBs	Whole	4.3	(Leney et al. 2006a)[c]
Green frogs (*Rana clamitans*)	Hibernation	M/F	Experimental	PCBs	Whole	1.4	(Angell and Haffner 2010)[c]
Fish							
Sockeye salmon (*Oncorhynchus nerka*)	Migration	M/F	Field	PCBs, PCDD/Fs	Muscle, gonad, liver	9.7	(DeBruyn et al. 2004)[b]
Europeans eel (*Anguilla anguilla* L)	Migration	F	Experimental	PCBs	Muscle	14.0	(Van Ginneken et al. 2009)[b]
Chinook salmon (*Oncorhynchus tshawytscha*)	Larval development	M/F	Experimental	PCBs, OCs	Whole	4.9	(Daley et al. 2012)[d]
Arctic Char (*Salvelinus alpinus*)	Overwintering	M/F	Experimental	PCBs	Liver, kidney	6.8	(Jorgensen et al. 1999)[d]
Yellow perch (*Perca flavescens*)	Incubating eggs	M/F	Experimental	PCBs	Whole	5.4	(Daley et al. 2009)[c]
Common sole (*Solea solea*)	Larval development	M/F	Experimental	PCBs	Whole	10.1	(Foekema et al. 2012)[d]
Yellow perch (*Perca flavescens*)	Overwintering	M/F	Experimental	PCBs	Whole	2.3	(Paterson et al. 2007a, b)[d]
Pacific salmon (*Oncorhynchus* spp)	Migration	M/F	Field	PCBs, OCs, PCDD/Fs	Muscle, gonad, liver	10	(Kelly et al. 2011)[d]
Birds							
Kittiwakes (*Rissa tridactyla*)	Reproduction	F	Field	PCBs	Liver, brain, fat	4.8	(Henriksen et al. 1996)[d]
Herring Gull (*Larus argetatus*)	Incubating eggs	M/F	Experimental	PCBs	Embryo	3.3	(Drouillard et al. 2003)[d]
Greater scaup (*Aythya marila*)	Overwintering	M	Field	PCBs, OCs	Muscle, fat pad	5.5	(Perkins and Barclay 1997)[d]
Common eiders (*Somateria mollisima*)	Incubation fast	F	Field	PCBs, OCs	Blood	6.1	(Bustnes et al. 2010)[d]
White Carneau pigeons (*Columba livia*)	Starvation	M/F	Experimental	PCBs	Blood, liver, kidney, brain, muscle, whole	5.7	(DeFreitas and Norstrom 1974)[d]

Mammals							
Harp seals (*Phoca groenlandica*)	Reproductive fast	F	Field/experimental	PCBs, OCs	Blood, blubber	7.2	(Lydersen et al. 2002)[d]
(*Zalophus californianus*)	Domoic acid fast	M/F	Field/experimental	PCBs, OCs, PBDEs	Blubber	2.5	(Hall et al. 2008)[d]
Polar bears (*Ursus maritimus*)	Summer fast	M/F	Field	PCBs, OCs	Fat	1.5	(Polischuk et al. 2002)[d]
Grizzly bears (*Ursus arctos horribilis*)	Hibernation	M/F	Field	PCBs, OCs, PBDEs	Fat	3.8	(Christensen et al. 2007)[d]
Elephant seals (*Mirounga angustirostris*)	Juvenile development	M/F	Field	PCBs	Blubber, blood	1.9	(Debier et al. 2006)[d]
Sea otters (*Enhydra lutris nereis*)	Infectious disease	M/F	Field	PCBs, OCs	Liver, kidney, brain	6.3	(Nakata et al. 1998)[d]
Humans (*Homo sapiens*)	Restricted diet	M/F	Field/experimental	PCBs, OCs	Blood	1.3	(Pelletier et al. 2002)[d]
Humans (*Homo sapiens*)	Restricted diet	M/F	Field/experimental	PCBs, OCs	Blood, fat	1.4	(Chevrier et al. 2000)[d]
Grey seals (*Halichoerus grypus*)	Lactation	F	Field	PCBs	Blood, blubber	2.5	(Debier et al. 2003)[d]
Grey seals (*Halichoerus grypus*)	Lactation	F	Field	PCBs, OCs	Blood, blubber	2.7	(Sormo et al. 2003)[d]

[a]Chemical acronyms: *PCBs* polychlorinated biphenyls, *OCs* organochlorines, *PCDD/Fs* polychlorinated dibenzodioxins/furans, *PBDEs* polybrominated diphenyl ethers
[b]BAmFs (bioamplification factors) were calculated or reported using a lipid equivalents ratio from the available data found in the corresponding citation
[c]BAmFs were calculated or reported using a fugacity ratio from the available data found in the corresponding citation
[d]BAmFs were calculated or reported using a lipid normalized ratio from the available data found in the corresponding citation

Chinook salmon are semelparous (characterized by a single reproductive episode before death), spawn in the fall, and allocate substantial maternal resources into eggs to enhance their survival during periods of prolonged ice cover (Bull et al. 1996; Kaitaranta and Ackman 1981; Russell et al. 1999b; Wiegand 1996). Following hatching, larval Chinook salmon tend to remain on gravel substrates and are nourished primarily by endogenous yolk reserves, because availability of external food remains low. These differences in the provisioning and timing of the use of maternal lipids produce important consequences for bioamplification during the early life stages of different fish species.

Daley et al. (2009) quantified the changes that occurred in proximate composition and PCB concentrations in yellow perch eggs during embryo development. These authors demonstrated a loss of egg dry mass over time and a decline in lipid content. Significantly, PCB fugacities quantified in yellow perch eggs at later stages of incubation were an average 2.7-fold (range: 1.8–5.4) higher than measured in newly fertilized eggs (Daley et al. 2009). For Chinook salmon eggs, no declines in lipid content were observed during the incubation period, and no concomitant bioamplification was observed (Daley et al. 2012). However, during the free swimming larval stage, juvenile Chinook salmon fry exhibited steady decreases in lipid content over time, which resulted in significant PCB bioamplification increases. For these fry, a maximum lipid-equivalent BAmF of 4.9 was determined by the end of yolk resorption (Daley et al. 2012). A similar magnitude of bioamplification has been observed in the early life stages of sole (*Solea solea*), whereby the lipid-normalized PCB concentrations peaked just prior to first feeding. The lipid-normalized concentrations in the late yolk sac larvae were approximately eightfold to tenfold higher than in the newly hatched larvae (Foekema et al. 2012).

Bioamplification-related increases in POP concentrations have also been observed during the development of juvenile grey (*Halichoerus grypus*) and northern elephant (*Mirounga angustirostris*) seals (Addison and Stobo 1993; Debier et al. 2006). Northern elephant seal pups are generally abruptly weaned from the mother, but can fast for up to 2.5 months and potentially lose up to 30% of their post-weaning body mass (Debier et al. 2006). During this period, lipid- normalized PCB concentrations quantified in blubber samples from elephant seal pups exhibit bioamplification, in addition to elevated blood serum PCB levels (Debier et al. 2006). Bioamplification-related increases in PCB concentrations have also been demonstrated during the post-weaning fast period in the blubber tissues of juvenile grey seals ranging from 0 to 13 months of age (Addison and Stobo 1993). Decreased POP concentrations were observed when grey seal pups resumed feeding (Addison and Stobo 1993). This was similar to the growth dilution observed for herring gull chicks and yellow perch larvae on initiation of feeding (Drouillard et al. 2003; Daley et al. 2009).

These studies demonstrate that bioamplification typically generates chemical concentrations that increase during embryo and juvenile development until independent external feeding is initiated by the animal. Such bioamplification trends can also be log K_{OW} dependent, whereby the more hydrophobic chemicals achieve the greatest BAmFs during larval development (Daley et al. 2012). Embryonic and larval/juvenile development also represents one of the periods in an animal's life

history, when they are most sensitive to the toxic effects from chemical exposure. As such, bioamplification could represent an important mechanism that mediates chemical toxicity during this critical developmental period (Daley et al. 2012; Foekema et al. 2012).

4.2 Bioamplification During Metamorphosis

During metamorphosis, several changes to an animal's biochemical, metabolic, and physiological functions may occur. In an experimental study using green frog (*Rana clamitans*) tadpoles, Leney et al. (2006a) dosed individuals with a PCB-Aroclor® mixture approximately three weeks prior to the onset of metamorphosis. Because tadpoles do not feed during metamorphosis, endogenous lipid mobilization was observed during this period, along with bioamplification of the PCB dose (Leney et al. 2006a). Bioamplification factors were maximized during tadpole metamorphosis by approximately 4.5-fold for the most hydrophobic PCB congeners (Leney et al. 2006a).

Aquatic insects have also demonstrated bioamplification during metamorphosis from pupae to larval life stages. Bartrons et al. (2007) reported an approximate threefold increase, when comparing mean dry weight POP concentrations between pupae and larval stages across four species of aquatic invertebrates. It was concluded that the increases in POP concentrations were due to the lack of feeding and subsequent loss of body weight during metamorphosis (Bartrons et al. 2007). During metamorphosis from juvenile instar to adult life stages, non-feeding emergent chironomids have been observed to increase PCB concentrations by approximately 4.6-fold, although this ratio was expressed on a fresh weight basis (Larsson 1984). Similarly, Harkey and Klaine (1992) documented increased concentrations of the pesticide chlordane in adult *Chironomus decorus* following metamorphosis. Given the wide range of invertebrate species that undergo multistage metamorphosis, it is likely that this phenomenon occurs commonly across this taxonomic group.

4.3 Bioamplification During Reproduction

Reproduction represents a substantial energy investment for most taxonomic groups and often encompasses substantial periods of feeding, fasting, and, for mammalian species, a lactational period that entails significant energetic costs. For example, female elephant seals follow a prolonged feeding period with a 3-month period that includes fasting, competition for mates and breeding (Schneider 2004). In some phocid species, up to 40% loss of body mass occurs during reproductive activities, in comparison to the non-breeding season (Lydersen et al. 2002). These species have a unique life history in that females undergo an extensive lactation period, which is consequently followed by molting, and both of these events incur

substantial energetic costs (Nilssen et al. 1995). For these individuals, the highest body condition indices occur prior to lactation and breeding (Lydersen et al. 2002). Individual females in poor physical condition during molting were determined to have blood PCB concentrations that were 7.2-fold higher than those measured from individuals having higher body lipid content (Lydersen et al. 2002). Increases in serum- and milk-PCB concentrations have also been documented in blood and milk samples collected from lactating female grey seals (Debier et al. 2003; Sørmo et al. 2003). Additionally, adult harp seals (*Phoca groenlandica*) that fasted over a 28-day period were observed to lose up to 24 kg of body mass and also exhibited significant increases in blood POP concentrations by the termination of the fasting period (Lydersen et al. 2002). In nature, weight losses that occur during reproduction are often compounded when the animal molts, which could lead to BAmFs higher than those reported above (Lydersen et al. 2002).

Several avian species, including common eiders (*Somateria mollissima*), kittiwakes (*Rissa tridactyla*), and Adelie penguins (*Pygoscelis adeliae*), experience lengthy fasting periods during reproduction (Bustnes et al. 2010; Henriksen et al. 1996; Subramanian et al. 1986). Female common eiders in Arctic regions have been demonstrated to lose approximately 25% of their body mass and 35% of lipid reserves during the egg incubation period (Bustnes et al. 2010). Similarly, female kittiwakes can lose up to 20% of their body mass from the pre-breeding to late chick rearing stages of reproduction (Henriksen et al. 1996). For these species, the bioamplification-related changes in lipid-normalized POP concentrations ranged from 1.7- to 8.2-fold across tissues, including blood, liver, brain, and adipose lipid reserves (Henriksen et al. 1996; Bustnes et al. 2010). Subramanian et al. (1986) indicated that maximum BAmFs of 3.5 and 2.8 can be achieved by male and female Adelie penguins, respectively, during this species reproductive fasting period. Subramanian et al. (1986) also observed similar bioamplification-related changes in POP concentrations among liver, muscle, and brain tissues in Adelie penguins during reproduction.

Reproductive activities also often include courtship rituals and rigorous competition between male individuals, in efforts to ensure mating success. In the mayfly genera *Hexagenia* spp., male individuals engage in intensive mating swarms that lead to significant reductions in lipid reserves between the sub-imago and imago life stages (Daley et al. 2011). Mayflies have a unique life history in that the majority of their lifespan is spent burrowed in lake and river sediments. Mayflies emerge from sediments as sub-imagos and rapidly molt into their final reproductive adult imago stage (Edmunds et al. 1976). Adult male Ephemeropteran mayfly species, including *H. Limbata* and *H. rigidia*, also do not feed following their emergence and rely exclusively on accumulated lipid reserves during their search for mates. Daley et al. (2011) demonstrated that during this reproductive flight, male individuals lose up to 50% of their lipid reserves, whereas females lose <10%. Further, lipid-normalized PCB-congener concentrations quantified in male mayflies were observed to bioamplify by roughly a factor of 2 during reproductive swarm events. This contrasts BAmFs of approximately 1 for PCB concentrations quantified in female mayflies which do not expend as much energy in reproductive swarms (Daley et al. 2011).

4.4 Bioamplification During Overwintering

In addition to the metabolic challenges associated with thermoregulation for both poikilotherms and homeotherms, reduced food availability often accompanies the extended cool–cold temperatures associated with winter months. For extreme latitude fish species such as Arctic charr (*Salvelinus alpinus*), lipid reserves can be reduced by up to 80% during the overwinter period (Jobling et al. 1998). Jorgensen et al. (1999) experimentally confirmed that PCB concentrations in the tissues of starved Arctic charr demonstrate bioamplification. Further, redistribution of the chemical from fat/muscle into liver and brain tissues occurred during overwintering (Jorgensen et al. 2002). Similar observations have been made for sole (*Solea solea*), whereby up to fourfold bioamplification of PCB concentrations in liver and muscle tissues occurred during experimental starvation trials and in wild collected overwintering fish (Boon and Duinker 1985). Overwintering mesocosm studies have also confirmed the bioamplification of PCBs by overwintering yellow perch (Paterson et al. 2007a, b). Specifically, PCB lipid-normalized bioamplification factors ranging from 1.7 to 2.3 were generated during the overwintering months. This bioamplification was consistent with a lack of chemical elimination and depletion of lipid reserves during the cold water period (Paterson et al. 2007a, b).

Avian and mammalian species, including the greater scaup (*Aythya mariya*), bald eagles (*Haliaeetus leucocephalus*), and Arctic fox (*Vulpes lagopus*), have also demonstrated POP bioamplification during the overwinter season. Seasonal lipid mobilization by greater scaup and bald eagles resulted in POP bioamplification factors in muscle and adipose tissues that were up to 5.5-fold during overwinter periods (Elliott et al. 1996; Perkins and Barclay 1997). Arctic foxes rely on sea bird forage during the spring and summer; however, as these prey items migrate from Arctic regions during the winter, individual foxes often face starvation (Fuglei and Oritsland 1999; Sonne et al. 2009). During winter starvation, a significant negative relationship between animal lipid content and POP concentrations was observed, which is consistent with POP bioamplification (Fuglei et al. 2007). Similar observations have also been made when comparing POP patterns quantified in winter-collected older lean foxes versus younger fatter individuals (Wang-Andersen et al. 1993).

4.5 Bioamplification During Hibernation

Hibernation is generally characterized as a behavioral and/or physiological mechanism invoked by species for enduring prolonged overwinter events and periods of low food availability. Current examples of hibernation-induced bioamplification include bat (Clark and Prouty 1977; Clark and Krynitsky 1983), amphibian (Angell and Haffner 2010), and bear species (Christensen et al. 2007), but is also likely to occur for the majority of animal taxa that undergo a state of hibernation, torpor, or estivation.

For bear species such as the grizzly (*Ursus arctos horribilis*), hibernation is referred to as pseudo-hibernation because the animal maintains a body temperature within a few degrees of normal; however, the potential for chemical elimination via defecation

and urination is minimized, because they are unlikely to feed (Hock 1960; Lyman et al 1982; Nelson 1978; Svihla and Bowman 1954). In a study of hibernating grizzly bears, there was an average 2.21 lipid-normalized concentration effect for ΣPCBs in post-hibernation compared to pre-hibernation bears (Christensen et al. 2007). For POPs such as dichloro-diphenyl-trichloroethane (DDT), which can be metabolized, no significant increases in chemical residue were demonstrated (Christensen et al. 2007).

Unlike other bear species, polar bears (*Ursus maritimus*) remain active over the winter months, while searching for prey during the ice cover season. However, polar bears are regarded to endure a "walking hibernation" or pseudo-hibernation (Nelson et al. 1983; Ramsay et al. 1991). This occurs during the summer months when animals experience lengthy periods of low food availability from the lack of ice cover (Chow et al. 2011). Polischuk et al. (2002) sampled polar bears in July and August and demonstrated a BAmF of approximately 1.3-fold for lipid-normalized ΣPCBs, compared to animals sampled in the winter from September to November. The highest BAmFs of 1.5 was determined for female bears with nursing cubs (Polischuk et al. 2002). Elevated levels of POPs have also been quantified in blood samples collected from polar bears during the summer months, indicating the potential mobilization of these chemicals from inert fat stores into the circulatory system (Knott et al. 2011; Polischuk et al. 1995, 2002).

Some of the earliest observations of POP bioamplification during hibernation were reported for a range of bat species (Clark and Prouty 1977; Clark and Krynitsky 1983). Hibernation in many bat species commonly occurs from early autumn to spring, and the animals typically rely on fat reserves to survive and recover during this period (Fenton and Barclay 1980). The depletion of lipid reserves during hibernation has been observed for big brown (*Eptesicus fuscus*), little brown (*Myotis lucifugus*), and eastern pipistrelle (*Pipistrellus flavus*) bats (Clark and Prouty 1977; Clark and Krynitsky 1983). Critically, concentrations of POPs, including the DDT metabolite dichloro-diphenyl-dichloroethylene (DDE), have been demonstrated to bioamplify significantly during this hibernation (Clark and Prouty 1977; Clark and Krynitsky 1983). Of particular significance, mortalities in bat populations have been observed coincident with animal arousal from hibernation, when lipid reserves are at their lowest, and thus, the potential for bioamplification is maximized (Clark 1981).

Northern latitude amphibian species also respond to harsh winter conditions by entering a hibernation state. Recently, Angell and Haffner (2010) sampled hibernating green frogs from October–January to quantify changes in PCB dose kinetics and animal lipid contents. The lipid content of frogs declined through the sampling period, with maximum BAmFs of 1.4 occurring for more recalcitrant hydrophobic ($\log K_{OW}$ >6.5) PCB congeners (Angell and Haffner 2010).

4.6 Bioamplification During Migration

Migration is a ubiquitous life strategy that is demonstrated in nearly all major taxonomic groups, including birds, mammals, fishes, reptiles, amphibians, and insects. Among these taxa, fishes and birds provide primary examples of extensive long

distance migrations that require energy demands from animals that are sufficient to bioamplify POPs.

Anadromous fish such as salmonid species often migrate long distances to return to natal streams and rivers to spawn. For example, the Yukon River Chinook salmon population is known to swim distances over 3,000 km during their migration (Beacham et al. 1989). Such extensive migrations have been demonstrated to deplete 90% of somatic lipid reserves in some individuals that return to spawning sites (Hendry and Berg 1999). Such extensive loss of somatic energy reserves has been demonstrated to bioamplify POPs, including PCBs, up to tenfold in migrating sockeye salmon (*Oncorhynchus nerka*) over the combined duration of the migration and spawning events (DeBruyn et al. 2004b; Ewald et al. 1998; Kelly et al. 2007b, 2011). Similar examples of POP bioamplification have been demonstrated for migrating Atlantic (*Salmo salar*) (Hansson et al. 2009) and Chinook salmon populations (Kelly et al. 2011). Of particular significance, the magnitude of PCB bioamplification by salmonid species is positively correlated with both migration distance and chemical log K_{OW} value (DeBruyn et al. 2004; Kelly et al. 2011). Similar to Pacific salmonids, the catadromous European eel (*Anguilla anguilla*) often returns to spawning grounds that are thousands of kilometers from feeding areas, and these animals tend to fast during migration (Olivereau and Olivereau 1997). This species can spend between 5 and 18 years in river- and coastal-feeding grounds prior to migrating to oceanic spawning grounds (Belpaire and Goemans 2007). Lipid-normalized concentrations of the organochlorine insecticide lindane have been quantified at a level of 9,255 ng/g, in pre-spawning European eel populations (Belpaire and Goemans 2007). Van Ginneken et al. (2009) demonstrated that the depletion of lipid reserves in more actively swimming European eels resulted in PCB congener bioamplification up to 14-fold higher than levels found in resting individuals. Eels also demonstrated little capacity for eliminating chemicals during such non-feeding events (Duursma et al 1991). Many Anguillid eels, such as the European and American eel (*Anguilla rostrata*) are at-risk species for conservation, and the very high POP concentrations and low lipid reserves have been identified as factors contributing to eel population declines (Belpaire and Goemans 2007).

Numerous bird populations undertake lengthy migrations. However, less is known about how bird migration influences bioamplification, mainly because of difficulties associated with measuring POP concentrations and body condition during migration events. Migration patterns among bird species also differ substantially, resulting in widely different energy demands. For many bird species, migration involves flight over relatively large food-limited areas, thus providing minimal opportunities for refueling (Klaassen 1996). Additionally, in larger non-gliding migratory species, active flight, rather than wind-assisted gliding, serves to more rapidly deplete energy reserves (Klaassen 1996). During such long distance migrations, wind direction and climate also affect metabolic costs. For example, headwinds increased the consumption of lipid stores (Colabuono et al. 2012; Piersma 2002). Such rapid depletion of lipid stores during migration has been observed to result in the redistribution of POPs among lipid, liver and muscle tissues

in Antarctic migratory species (Colabuono et al. 2012). Critically, overall animal body condition, as indicated by lipid content and starvation status, have been determined to be important factors in the redistribution of POPs in animal tissues during bird migration (Colabuono et al. 2012; Sodergren and Ulfstrand 1972).

4.7 Other Events Leading to Bioamplification

For some animal species, aphagia often occurs with the onset of disease, and this condition can generate the negative energy imbalance that is consistent with energetic bottlenecks and weight loss. For example, California sea lions (*Zalophus californianus*) exposed to the domoic acid neurotoxin cease feeding and can lose substantial body mass and blubber content (Hall et al. 2008). During a 12-day aphagia period, individuals exposed to this neurotoxin lost approximately 16% of their body mass and exhibited bioamplification (of PCBs, DDT, brominated flame retardants, and other POP compounds) in blubber tissues (Hall et al. 2008). Stranded sea otters (*Enhydra lutris nereis*), which died from disease and emaciation, exhibited higher lipid-normalized DDT concentrations than did animals that died from acute trauma (Nakata et al. 1998). Similar patterns of POP bioamplification have been observed in stranded dolphins, relative to those caught as by-catch (Chou et al. 2004). The patterns of PCB bioamplification were consistent with higher levels of lipid mobilization in the diseased and starving animals that were found stranded (Chou et al. 2004). Evidence for POP bioamplification has also been observed in diseased black-backed gulls (*Larus fuscus fuscus*) and little brown bats (Hario et al. 2004; Kannan et al. 2010). In addition, weight loss and starvation experiments have demonstrated POP bioamplification in humans (Chevrier et al. 2000; Pelletier et al. 2002; Tremblay et al. 2004; Walford et al. 1999), birds (Defreitas and Norstrom 1974; Ecobichon and Saschenbrecker 1969; Stickel et al. 1984), fish (Antunes et al. 2007), and rodents (Dale et al. 1962; Jandacek et al. 2005; Ohmiya and Nakai 1977).

5 Modelling POP Bioamplification

Non-steady state bioaccumulation models, and in some cases multi-life stage bioaccumulation models, have been described for POP compounds in marine mammals (Czub and McLachlan 2007; Hickie et al. 1999, 2000, 2005, 2007; Yordy et al. 2010), birds (Clark et al. 1987, 1988; Drouillard et al. 2003; Norstrom et al. 1986a, 2007), and fish (Drouillard et al. 2009; Foekema et al. 2012; Ng and Gray 2009; Sijm et al. 1992). However, relatively few of the studies just cited were focused explicitly on interpreting bioamplification peaks resulting from model simulations. Drouillard et al. (2003) used a non-steady state embryo bioaccumulation model to contrast differences in lipid-normalized PCB concentrations in herring gull embryos through

incubation. The above simulation demonstrated that pipping-aged chicks can achieve bioamplification factors of 3.1 and 1.5, compared to fresh eggs and laying females, respectively. Foekema et al. (2012) applied an analogous approach to model hydrophobic POP bioaccumulation in the embryo stage of a fish, the common sole (*Solea solea*). Based on their simulations, the authors concluded that at the end of the yolk-sac stage, sole larvae can achieve bioamplification factors of between 2 and 4, compared to spawning parent fish for compounds having log K_{OW} values exceeding 5.

There are few examples, in which non-steady state bioaccumulation models have been applied to adult life stages that incorporate realistic seasonal changes in whole body lipids, and assess the impact of this on POPs bioamplification. Norstrom et al. (2007) highlighted the importance of including seasonal changes in lipid content as a model variable, because of the close interaction that exists between whole body lipid content and POP toxicokinetics. Incorporating the effects of seasonal changes on lipid content is particularly important as it relates to chemical elimination by animals. For example, Clark et al. (1988) used the herring gull bioenergetic and toxicokinetic model (described in Clark et al. 1987; Norstrom et al. 1986a, b) to predict pronounced seasonal changes in dieldrin and mirex chemical fugacities as they related to decreases in adult bird fat stores that occur each spring. Similarly, Czub and McLachlan (2007) applied a non-steady state bioaccumulation model to POPs in ringed seals. This model predicted seasonal bioamplification factors of 2 or more in seals that resulted from the blubber loss that occurs during molting in the spring and early summer. Drouillard et al. (2009) established a non-steady state model for yellow perch that accounted for seasonal lipid changes and its effect on PCB depuration kinetics. Importantly, this last study showed that winter weight loss, as experienced by aquaculture-reared yellow perch, exceeded the rate of PCB elimination, enabling bioamplification to occur.

Model Simulations. To further demonstrate the application of multi-life stage, non-steady state bioaccumulation models to predict bioamplification, two case studies are presented in the appendices for a fish and bird using previously reported models. For fish, a modified version of the yellow perch bioenergetic and toxicokinetics model reported by Drouillard et al. (2009) was adopted. The model was extended to include growth over most of the lifespan (age 1–9) of this species. Yellow perch ages as high as 7–9 years have been reported for North American populations, including the populations inhabiting the Great Lakes (Scott and Crossman 1998). Growth rates, temperature-dependent specific growth and temperature-dependent changes in whole body lipid content and lean dry protein were incorporated as described in Appendix 1. The fish bioenergetics sub-model used proximate composition, growth, and body size data in conjunction with water temperatures to predict daily food consumption and gill ventilation rates as described by Drouillard et al. (2009). Since the Drouillard et al. (2009) model was limited to describing chemical elimination, the model was modified to incorporate chemical uptake from water and food, by using equations described by Arnot and Gobas (2004). Simulations were initiated using a 1-year-old male fish that was assumed to be in equilibrium with water for a chemical having a log K_{OW} of 6.5. The chemical was assumed to not be

subject to biotransformation by fish. Fish growth was simulated over an 8-year period, with fish fed a diet of constant proximate composition, energy density, and chemical concentration throughout the simulation. The chemical concentration in the diet was set such that the diet was in equilibrium with an assumed constant water concentration. Two simulation scenarios were modeled. In the baseline scenario, a constant temperature of 21 °C was maintained throughout the simulation, and hence, did not allow for seasonal weight loss to occur. The second scenario, referred to as the dynamic temperature scenario, allowed temperature to vary by season according to an annually repeating temperature profile recorded for Southern Ontario, Canada. Appendix 1 provides a full description of the yellow perch bioaccumulation model, parameters and algorithms used for model calculations.

For birds, a modified version of the herring gull bioenergetic and toxicokinetic model as described by Norstrom et al. (2007) was utilized (Appendix 2). The model was formulated to simulate what would occur in a male bird to avoid having to incorporate depuration of maternal residues to eggs, and to predict maximum bioamplification factors for this species. The model was adapted to predict chemical residues across multiple life stages, commencing with a pipping chick, followed by chick growth through fledging, to a subadult male life stage and reproductively active adult life stage over an 8-year simulation period. The bioenergetic portion of the model predicted daily growth, proximate composition, and feeding rate of a male bird as described in Norstrom et al. (1986b). The toxicokinetic sub-model predicted chemical uptake from food and chemical elimination at daily intervals as described in Clark et al. (1987). A slight modification to the model was that the plasma/fat partition coefficient (K_{PF}) was redefined as a plasma/lipid equivalent partition coefficient to be consistent with the yellow perch model. This consideration reflects the current understanding of chemical partitioning within organisms (Debruyn and Gobas 2007). The values for K_{PF} and the plasma clearance constant (k'_{pc}) were chosen from those reported for Mirex to provide a non-biotransformed, highly hydrophobic chemical comparable to the fish simulations. As in the case of the yellow perch model, two simulations were performed. In the baseline simulation, temperature and photoperiod were kept constant at 21 °C and 12 h/d across seasons and years. The seasonal scenario relied on an annually repeating temperature and photoperiod profile from Lake Ontario during 1997. The model was initialized using a fresh egg concentration predicted from a 10-year old female adult model simulation (Clark et al. 1988). This female bird was fed a constant diet of the same concentration and energy density as had been used for male simulations. The female was also subjected to equivalent temperature and photoperiod profiles. Bioamplification of fresh egg residues in the pipping embryo was estimated by multiplying the fresh-egg lipid-equivalent concentration by a factor of 3.1 as suggested by Drouillard et al. (2003). The bird was subsequently modeled to feed on a constant food source of similar proximate composition, energy density and chemical concentration over the duration of the study. A full description of model parameters and algorithms for the herring gull simulations are presented in Appendix 2.

In Fig. 1, we summarize the yellow perch model output for the baseline and seasonal temperature scenarios. Body weight of the 1–8-year-old fish varied between

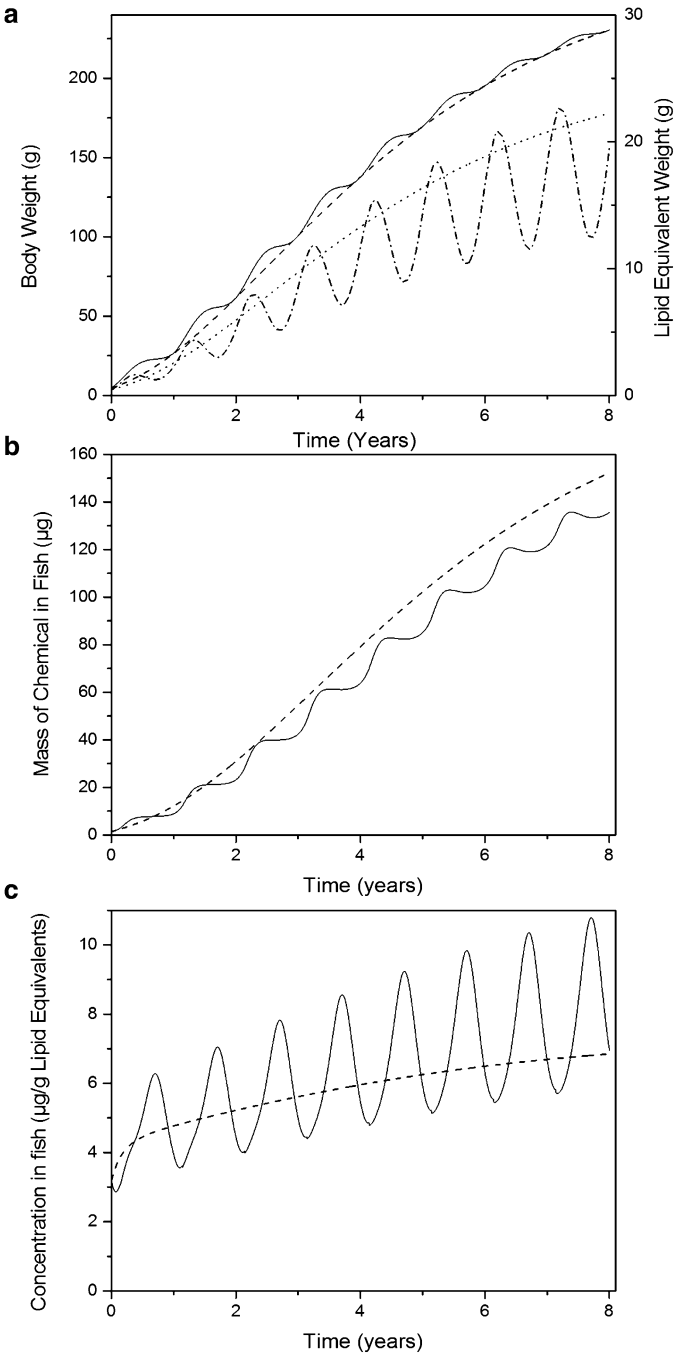

Fig. 1 Yellow perch model simulations for baseline and seasonal temperature scenarios. (**a**) Body weight (g) is simulated from a baseline constant temperature (*dashed line*) and a dynamic temperature scenario (*solid line*). Lipid-equivalents (g) are simulated for a baseline constant temperature (*dotted line*) and dynamic temperature scenario (*long dash-dot*). (**b**) Mass of chemical in the fish (µg) is presented for the baseline constant temperature (*dotted line*) and dynamic temperature scenario (*solid line*). (**c**) Chemical concentration (ng/g lipid-equivalents) is simulated for a baseline constant temperature (*dotted line*) and dynamic temperature scenario (*solid line*)

4.8 and 230 g for the two scenarios (Fig. 1a). The upper limit of this range is similar to the 257 g body weight value reported for 8+-year-old yellow perch collected from the Bay of Quinte, Ontario, Canada (Scott and Crossman 1998). For the dynamic temperature scenario, body weights were marginally higher in the summer months, as a result of the temperature dependence of fish feeding rates and growth during warm water seasons (Kitchell et al. 1977). In contrast, winter growth approached zero. Differences in growth between simulations were more pronounced when comparing model predictions of fish whole-body lipid-equivalent weights over time. The baseline simulation produced lipid-equivalent weight estimates at the upper range of those predicted during the summer of the dynamic temperature scenario. These upper range estimates resulted from the high constant temperature used in the simulation. Lipid-equivalent weights in the baseline scenario mirrored body weight trends, whereas % lipid was constant at 8.6%. In the seasonal scenario, lipid-equivalent weights showed strong seasonal cycles. In each year of the simulation, the % lipid decreased to a minimum value of 4.3% in the winter and to a maximum value of 9.3% in the summer. These values corresponded to a 2.1-fold difference in lipid content on a per annum basis.

Changes in the total fish body burden of chemical from the two scenarios are provided in Fig. 1b. Fish consumed less food during the winter and had lower lipid-equivalent weights in the dynamic temperature simulation. Consequently, the total chemical mass accumulated by fish under the seasonal simulation was lower than that observed for the baseline scenario. The magnitude of these differences also increased with fish age. Figure 1c contrasts lipid-equivalent concentrations of the chemical in fish under the two scenarios. Lipid-equivalent concentrations were predicted to increase with age over the duration of the baseline scenario simulation. This observation is consistent with non-steady state bioaccumulation. This occurred since fish did not reach their maximum size as predicted by the von Bertalanffy growth model. The dynamic temperature scenario predicted pronounced seasonal oscillations for chemical concentrations in fish that were opposite those observed for whole body lipid-equivalents. Specifically, lipid-equivalent concentrations peaked on Feb. 1 of each simulation year, coincident with animal minima for lipid-equivalent weights (Fig. 1a). In contrast, the lowest annual lipid-equivalent concentrations occurred on July 17th of each year, when lipid-equivalent weights were maximized.

In Table 2, we summarize the metrics for comparing model outputs from the yellow perch constant and dynamic temperature scenarios. Both of these scenarios predicted a non-steady state for fish over the simulation duration. Thus, temporal changes in chemical mass balance and lipid-equivalent concentrations are required to demonstrate the occurrence of bioamplification. The first column of Table 2 describes the ratio of maximum to minimum chemical mass (ng) in the fish for each year of the simulations. This mass balance ratio exceeded 1 in all simulation years and tended to be higher for the dynamic temperature scenario. BAmF values exceeded 1 in all simulations and approached a near constant value (1.89–1.90) for the later years of the dynamic temperature scenario. Moreover, BAmF values exceeded the chemical mass balance ratios for years 3–8 during this scenario, validating the occurrence of bioamplification. Bioamplification occurred despite the fact that the organism was

Table 2 Model predicted changes in age specific mass balance, lipid equivalents, and BAmFs in yellow perch over the simulation duration

Year interval	ΔX_{fish} max/min chemical mass (ng) in fish over a given year	BAmF max/min lipid equivalents concentration in fish over a given year	Across simulation ratio of the peak lipid equivalent concentration between scenarios[a]
0–1	6.77 (8.27)[b]	2.19 (1.49)[b]	1.36
1–2	2.61 (2.54)	1.98 (1.09)	1.38
2–3	1.82 (1.76)	1.96 (1.08)	1.42
3–4	1.50 (1.45)	1.95 (1.06)	1.46
4–5	1.33 (1.29)	1.93 (1.05)	1.49
5–6	1.23 (1.20)	1.91 (1.04)	1.53
6–7	1.16 (1.14)	1.90 (1.03)	1.56
7–8	1.12 (1.09)	1.89 (1.02)	1.59

[a]Expresses the ratio of the maximum lipid equivalent concentration determined in a given year for the dynamic temperature simulation scenario to the lipid equivalent concentration determined on the same day for the constant temperature scenario

[b]First number corresponds to the dynamic temperature scenario. Value in parentheses corresponds to the constant temperature scenario

still in the uptake stage of the bioaccumulation curve (Fig. 1b). In contrast, BAmF values for the constant temperature scenario were close to 1 (1.02) by the last simulation year and did not exceed the chemical mass balance ratio. This demonstrates that bioamplification did not occur during the constant temperature scenario.

Herring gull model outputs are provided in Fig. 2. Temporal changes in whole body and lipid-equivalent weights are depicted in Fig. 2a. Juveniles grew rapidly during the first 90 days of the simulations. Under the dynamic temperature scenario, body weight and lipid-equivalent weights fluctuated according to an annual cycle each year following fledging. After the first simulation year, herring gull whole body and lipid-equivalent weights changed annually by 1.07- and 1.67-fold, respectively. Seasonal changes in herring gull lipid-equivalent weights were opposite those observed for fish. Specifically, herring gull lipid-equivalent maxima occurred in the winter while minima occurred during the summer. Lipid-equivalent weights were always higher in the dynamic temperature scenario, relative to the baseline simulation, due to the high temperature (21 °C) selected for constant temperature simulation.

Figure 2b contrasts the magnitude of chemical mass accumulated by birds under the two scenarios. For the dynamic temperature scenario, male birds accumulated higher chemical mass, relative to that predicted under the baseline scenario. This occurred because of the higher lipid content predicted for birds under the dynamic temperature scenario. Bird chemical mass approached an asymptote between years 2 and 4 of the simulation, with seasonal oscillations in chemical mass occurring after year 4. These oscillations were associated with courtship feeding and chick rearing costs that caused seasonal changes in animal food consumption rates. These behaviors contribute to increased chemical uptake followed by lags in elimination, with a gradual return to steady state by the following year. Unlike fish, rapid early growth by fledging chicks facilitated the steady state condition for the chemical

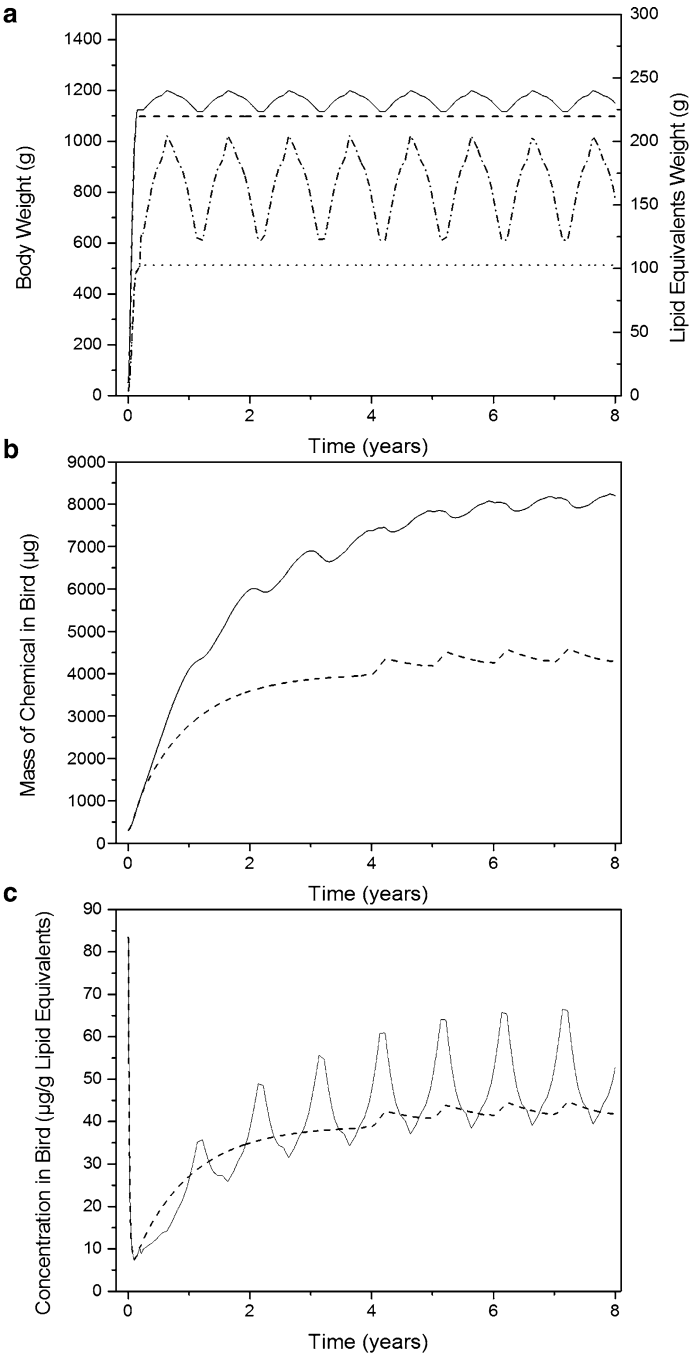

Fig. 2 Herring-gull model-simulations for baseline and seasonal temperature scenarios. (**a**) Body weight (g) is simulated from a baseline constant temperature (*dashed line*) and a dynamic temperature scenario (*solid line*). Lipid equivalents (g) are simulated for a baseline constant temperature (*dotted line*) and dynamic temperature scenario (*long dash-dot*). (**b**) Mass of chemical in the fish (µg) is presented for the baseline constant temperature (*dotted line*) and dynamic temperature scenario (*solid line*) (**c**) Chemical concentration (ng/g lipid-equivalents) is simulated for a baseline constant temperature (*dotted line*) and dynamic temperature scenario (*solid line*)

Table 3 Model predicted changes in age specific mass balance, lipid equivalents, and BAmFs in male herring gulls over the simulation duration

Year interval	ΔX_{fish} max/min chemical mass (ng) in fish over a given year	BAmF max/min lipid equivalents concentration in fish over a given year	Across simulation ratio of the peak lipid equivalent concentration between scenarios[a]
0–1	11.17 (13.92)[b]	12.76 (8.65)[b]	1.88
1–2	1.45 (1.30)	1.48 (1.30)	1.22
2–3	1.16 (1.08)	1.55 (1.08)	1.38
3–4	1.11 (1.03)	1.62 (1.03)	1.47
4–5	1.07 (1.09)	1.64(1.09)	1.45
5–6	1.05 (1.08)	1.67 (1.08)	1.51
6–7	1.04 (1.07)	1.68 (1.07)	1.52
7–8	1.04 (1.07)	1.69 (1.07)	1.53

[a]Expresses the ratio of the maximum lipid equivalent concentration determined in a given year for the dynamic temperature simulation scenario to the lipid equivalent concentration determined on the same day for the constant temperature scenario

[b]First number corresponds to the dynamic temperature scenario. Value in parentheses corresponds to the constant temperature scenario

under the baseline scenario. In contrast, steady state was not achieved until 5 years of age for birds under the dynamic temperature scenario. Greater seasonal oscillations in the magnitude and duration of chemical mass balance under the dynamic temperature scenario were attributed to temperature-dependent changes in feeding rates and reproduction-associated foraging costs occurring after year 4.

Trends in lipid-equivalent chemical concentrations throughout the herring gull life history are provided in Fig. 2c. Distinct bioamplification occurs for pipping chicks during the first 90 days of growth under both temperature scenarios. Under the baseline scenario, pipping chicks commenced with a lipid-equivalent concentration of 53.85 μg/g, which exceeds the maximum achieved by adult males (44.68 μg/g) by 1.2-fold. For the dynamic temperature scenario, pipping chicks had an initial lipid-equivalent concentration of 101.1 μg/g, which was 1.5-fold higher than the maximum predicted for adult males (66.9 μg/g). Although chemical mass in birds continued to increase with time (Fig. 2b), rapid growth dilution and a diet switch from highly contaminated yolk lipids to less contaminated external prey resulted in a precipitous drop in chick lipid-equivalent concentrations by day 37 (7.92 μg/g). These results demonstrate the importance of temporal lipid dynamics on chemical bioamplification in adult birds, chicks and at the time of maternal transfer.

In Table 3, we summarize the simulation metrics for the herring gull chemical concentrations, under the constant and dynamic temperature scenarios. BAmF values did not exceed the chemical mass balance ratio during any simulation year of the baseline scenario. Moreover, excluding year 1, BAmF values and chemical mass balance ratios were equal for each simulation year, suggesting an absence of bioamplification for older birds under this simulation. For the dynamic temperature simulation, BAmF values exceeded chemical mass balance ratios and progressively increased from 1.48 to 1.69 from years 1 to 8. These results confirm the occurrence of bioamplification in herring gulls under the dynamic temperature scenario.

Both models demonstrated the capacity of fish and birds to bioamplify hydrophobic, negligibly transformed chemicals throughout their life histories. This occurs primarily due to age-related changes in growth and seasonal weight loss. The temporal bioamplification trends for fish and birds were different, because fish feed less in winter and have reduced body fat content, whereas birds increase food intake, thereby enhancing fat deposits in winter. These differences are expected to occur, because ectothermic and endothermic species respond differently to low temperature exposures. Under the dynamic temperature scenario, BAmFs for both fish and birds exceeded the maximum ratio of chemical mass balance by simulation years 7–8. These results confirm that bioamplification occurred as it is defined in this review. Specifically, the rate of weight loss exceeded that for chemical depuration. For birds, bioamplification patterns were complex across the life stages included in the simulations. Pipping chicks exhibited a pronounced bioamplification peak during early growth, followed by reduced bioamplification events that were associated with temporal changes in subadult foraging costs and reproductive activities for adult birds. Similar bioamplification peaks are likely to be present in pre-hatched yellow perch embryos as described by Daley et al. (2009) and modeled in larval sole by Foekema et al. (2012). However, such simulations were not included in the current study owing to the absence of empirical information that described larval fish growth and proximate composition for the first simulation year. Additional factors (e.g., spawning costs related to mate competition and/or changes in food availability) probably further contributed complexity to the fish bioaccumulation curve. However, these factors were not included in the model structure.

Additional research during the full life cycle of different species would prove beneficial for identifying critical exposure periods to hydrophobic chemicals that are associated with bioamplification events. Development of such models requires a comprehensive knowledge of changes in animal bioenergetics, proximate composition, and food types and availability that occur at both seasonal and annual temporal scales. Insights into other toxicokinetic parameters (e.g., chemical exchange efficiency terms related to dietary assimilation, uptake and depuration across gills, and organism/fecal exchange) are also critical to establishing such a model structure. Although the theory behind extrapolating toxicokinetic parameters to multiple organisms, based on chemical attributes, is relatively well established, gaps do remain in our understanding of age and diet-related effects on such toxicokinetic parameters (Arnot and Gobas 2004). In contrast, limited empirical data are available for describing the physiological and proximate composition characteristics of species across a range of natural habitats and over multiple life stages. Such paucity of information hinders the development of full life cycle chemical bioaccumulation as exemplified in this review. Finally, it should be noted that field sampling rarely considers seasonal dynamics in animal lipid content, when timing of animal collection is arranged. Seasonally staggered sampling programs are required to track bioamplification over seasonal temperature cycles. However, most temporal biomonitoring programs sample animals during restricted time periods (e.g., open water, summer months), because of sampling logistics and the need to characterize interannual temporal chemical bioaccumulation trends (Bhavsar et al. 2010; Gewurtz et al. 2011; Richman et al. 2011; Roose et al. 1998).

6 Implications of Bioamplification

Several of the case studies outlined in Sect. 4 demonstrate a central consequence of bioamplification: POP residues in the animal are redistributed from metabolically inert lipid reserves to more toxicologically sensitive tissues. Loss of animal lipid reserves has been associated with proportional increases in xenobiotic chemical concentrations in blood, liver, muscle, and brain tissues (Bustnes et al. 2010, 2012; Debier et al. 2003, 2006; Henriksen et al. 1996; Jørgensen et al. 1999, 2002; Lydersen et al. 2002; Perkins and Barclay 1997; Subramanian et al. 1986). For example, DeFreitas and Norstrom (1974) starved pigeons for 7 days and observed a net mass transfer of PCBs from adipose into brain, liver, and muscle tissues. Henriksen et al. (1996) showed a steady decrease in body mass and lipids for breeding kittiwakes, which resulted in a quadrupling of PCB concentrations in brain tissue. Such changes occur because much of an animal's capacity for chemical bioaccumulation is defined by the mass of adipose stores and it is these tissues that experience the greatest decreases during weight loss. Consequently, a twofold decrease in animal partitioning capacity causes an equivalent increase in chemical fugacity. This leads to commensurate increases in chemical wet weight concentrations in blood and other lean tissues. Furthermore, lean tissue POP concentrations change rapidly following weight loss events, because the time required to achieve inter-tissue equilibrium is short (~1 week; Braune and Norstrom 1989; Clark et al. 1987; Norstrom et al. 1986a), despite the time being long for the organism to achieve steady state with its environment (Drouillard et al. 2001). For a more detailed explanation of how toxicokinetic processes regulate target site concentrations and the mechanisms of toxic action of POPs, readers are referred to the review articles of Escher et al. (2011), McCarty et al. (2011) and McElroy et al. (2011).

POP residues in blood are generally more available to target organs than those present in adipose stores, and thus blood residues pose greater toxicological risk (Knott et al. 2011). Studies involving insects, fish, and mammals have shown significant positive relationships between animal lipid content and the LD_{50} value for chemicals, indicating that toxicity increases with a decreasing animal lipid content (Geyer et al. 1990, 1993). Birds have been shown to experience enhanced POP toxicity following periods of dramatic weight loss (Ecobichon and Saschenbrecker 1969; Gabrielsen et al. 1995; Stickel and Stickel 1969). Van Velzen et al. (1972) observed that birds exposed to DDT doses from 100 to 300 μg/g, or subjected to weight loss from reduced food availability, exhibited no mortality. However, the combined effects of weight loss and DDT exposure caused significant mortality in brown-headed cowbirds (*Molothrus ater*). Fish having a low body lipid content (and poor condition) have been demonstrated to experience greater negative effects from PCB exposure (25–2,500 μg/kg food/day) than those having a higher lipid content and better condition (Quabius et al. 2000). These studies emphasize that the toxicity experienced by animals from POP exposure is best correlated to chemical fugacity rather than the whole body or tissue specific wet weight concentration.

POP bioamplification has the potential to modify chemical biotransformation rates, thereby enhancing toxic metabolite formation via first and second order kinetic

processes. Bioamplification also has the potential to alter POP bioaccumulation signatures in the animal's tissues (Boon et al. 1989; Walker 1990). For example, the redistribution of PCBs from deep blubber layers into the bloodstream of bottlenose dolphins was suggested to induce cytochrome P450 mono-oxygenases, leading to enhanced production of PCB metabolites (Montie et al. 2008). As discussed in Sect. 4.4, Jorgensen et al. (1999, 2002) studied overwinter emaciation in Arctic charr and saw an increase in PCB concentrations in more sensitive tissues (e.g., kidney and brain). This long-term food deprivation in overwintering charr also led to marked increases in biomarker responses during this period of PCB redistribution. Leney et al. (2006b) demonstrated the onset of PCB biotransformation in green frogs immediately following metamorphosis, a period when bioamplification is maximized for this species. However, it was not determined whether biotransformation was a consequence of bioamplification, or was from the ontogenetic changes associated with metamorphosis (Leney et al. 2006b). Christensen et al. (2007) reported that fasting animals, such as hibernating bears, experience prolonged exposure to toxic biotransformation products, from reduced capacity to eliminate them via urine and fecal egestion during this dormant state. Unfortunately, the information available is too limited to draw general conclusions on the specific interactions that take place between POP bioamplification, chemical biotransformation rates, and metabolite-mediated toxicity responses.

Because there are many bioenergetic bottlenecks at critical and highly sensitive periods of an animal's life cycle, bioamplification of POPs may increase chemical toxicity during these susceptible periods. Bioenergetic imbalances and associated weight loss events are predicted to increase stress and enhance possibilities of chemical/stress toxicity interactions (Fuglei et al. 2007; Knott et al. 2011). For example, several POPs are known to interfere with behavioral responses such as predator avoidance (Schulz and Dabrowski 2001; Weis and Weis 1987). Therefore, bioamplification of POPs during larval and/or fry development may reduce the capacity for predator avoidance, when these animals become free-swimming individuals and are more susceptible to predation. Further, ontogenetic shifts from endogenous to exogenous food resources are often associated with elevated mortality. Thus, bioamplification could potentially augment mortality at this critical period for larval fish. While stranded cetaceans often have higher total POP burdens than healthy animals do, it is unknown what role bioamplification plays in such mortalities (Chou et al. 2004). Amphibian metamorphosis represents a period of substantive changes in gene transcription and translational activities, in addition to significant physiological and metabolic reorganization (Kawahara et al. 1991). Subsequently, the potential for chemical interference during gene expression is higher during metamorphosis than during other life stages.

7 Conclusions

In this review, we have demonstrated that bioenergetic bottlenecks and environmental stressors influence POP exposure dynamics for many taxonomic groups that utilize different life history strategies. The main conclusions of this review are:

1. Bioamplification occurs when an animal loses body mass and chemical partitioning capacity at a faster rate than it can eliminate contaminants.

   Bioamplification, explicitly, is a non-equilibrium, non-steady state process, in which chemical residues in animal tissues become concentrated from reductions in chemical partitioning capacity that occur due to rapid loss of body lipids, without a commensurate loss of chemical mass.
2. Bioamplification leads to the mobilization of POPs from inert storage sites (e.g., adipose tissue) to other more sensitive tissues.

   A major implication of bioamplification is that it increases chemical fugacity in the animal's tissues. Several case studies demonstrate that this increase in fugacity results in the redistribution of contaminants from inert lipid stores (adipose) to more toxicologically sensitive tissues.
3. Bioamplification often occurs during sensitive life stages in the animal's life history.

   We have demonstrated that bioamplification often produces enhanced POP fugacities and tissue-specific chemical concentrations at critical periods in an animal's life history. Common critical behavioral, ontogenetic and physiological events, when bioamplification has been demonstrated, include embryo development, juvenile life stages, metamorphosis, reproduction, migration, overwintering, hibernation, and disease.
4. As a bioaccumulation process, bioamplification is additive to bioconcentration and biomagnification mechanisms of chemical exposure.

   As outlined in model simulations (Sect. 5), bioamplification can result in animals achieving the same magnitude of chemical concentrations predicted by steady state bioaccumulation models, prior to the animal actually achieving steady state with its exposure media (Figs. 1c and 2c). Bioamplification can increase the chemical concentration in an animal to levels that exceed the maximum concentration predicted for a given species by steady-state biomagnification models.
5. Examples of bioamplification of POPs can be found across the animal kingdom.

   Case studies of bioamplification are presented and include examples across a range of animal taxa including invertebrates, amphibians, fishes, birds, and mammals. Occasionally, BAmFs were observed to approach or exceed BMFs reported for POPs compounds. For example, observed BMFs for POPs in fish species often range from 5 to 10, whereas migrating salmon and eels have been shown to achieve BAmF's that exceed 10 (Table 1).

8 Future Directions

Bioamplification results in elevated POP fugacities and chemical concentrations during critical periods of the life history of many animal species. Consequently, understanding the dynamics of bioamplification and how behavioral, ontogenetic, and physiological changes during an animal's life history alter critical tissue

residues is important to bioaccumulation and risk assessment studies. Unfortunately, bioamplification is rarely considered in such studies. Most POP bioaccumulation models fail to fully consider the full scope of ecological, climatic, and physiological variables that regulate POP kinetics and bioaccumulation. In recent years, several authors have called for acquiring more robust datasets and for integrating more thorough life history information, as means to better calibrate and validate models (DeBruyn and Gobas 2006; Muir and de Wit 2010; Ng and Gray 2009; Norstrom et al. 2007). In our view, the major data gaps that require attention in future bioamplification research include the following:

1. Parameterization of life-stage specific toxicokinetic parameters and mapping their interactions with changing environmental conditions.
2. Understanding seasonal and life-stage specific growth, weight loss, and proximate composition changes under realistic environmental conditions.
3. Investigating the influence of multiple stressors (e.g., habitat alterations, climate change, species invasions, etc.) on growth, weight loss, and proximate composition in a given species.
4. Development of full lifecycle (embryo to adult) non-steady state bioaccumulation models.

Addressing these data gaps is not only essential for understanding and predicting POP bioaccumulation and biomagnification in food webs, but also for protecting wildlife, ecosystem, and human health.

9 Summary

Persistent organic pollutant bioaccumulation models have generally been formulated to predict bioconcentration and biomagnification. A third bioaccumulation process that can mediate chemical fugacity in an organism is bioamplification. Bioamplification occurs when an organism loses body weight and the chemical partitioning capacity occurs at a rate that is faster than the chemical can be eliminated. Although bioamplification has not been widely recognized as a bioaccumulation process, the potential consequences of this process are significant. Bioamplification causes an increase in chemical fugacity in the animal's tissues and results in the redistribution of contaminants from inert storage sites to more toxicologically sensitive tissues. By reviewing laboratory and field studies, we have shown in this paper that bioamplification occurs across taxonomic groups that include, invertebrates, amphibians, fishes, birds, and mammals. Two case studies are presented, and constitute multi-life stage non-steady state bioaccumulation models calibrated for yellow perch and herring gulls. These case studies were used to demonstrate that bioamplification is predicted to occur under realistic scenarios of animal growth and seasonal weight loss. Bioamplification greatly enhances POP concentrations and chemical fugacities during critical physiological and behavioral events in an animal's life history, e.g., embryo development, juvenile stages, metamorphosis,

reproduction, migration, overwintering, hibernation, and disease. Consequently, understanding the dynamics of bioamplification, and how different life history scenarios can alter tissue residues, may be helpful and important in assessing wildlife hazards and risks.

10 Appendix 1: Description of the Yellow Perch Model and Associated Simulations

Simulations were performed by finite difference, using a daily time step. The model was set up using a Microsoft Excel spreadsheet, and the calculation algorithms and/or constants for each variable of the model are summarized in Table 4. The model was initialized by assuming that day 1 corresponded to a 1-year-old fish (365 days old) hatched on May 20 of the previous year. The model was initialized at this life stage, because of a lack of data on growth, proximate composition changes and chemical toxicokinetics in larvae fish during the first year. The model was run for 2,920 days (i.e., 8 years from the simulation initialization). In the simulations, fish growth was allowed to change as a function of age, following the precedent of a von Bertalanffy model fitted to 22 North American populations of yellow perch (Jackson et al. 2008). The von Bertalanffy model was used to predict the length (cm) of fish at a given age (in days) for the constant temperature scenario. Body length (cm) was converted to a body weight (g) value, by using a linear regression equation fitted to the $\log_{10}$ of body length versus $\log_{10}$ of body weight (this approach relied on unpublished data that was generated for aquaculture-reared yellow perch; see Table 4).

For the dynamic temperature scenario, growth rates from the baseline simulations were further modified to make growth rates temperature dependent, whereas overall growth rates generally matched those of the constant temperature simulation. The modifications to the basic growth model are described as follows. On May 20 of each year (i.e., reflecting the assumed birthday of the fish), the body weight of the fish was set to be equal to the body weight estimated for the constant temperature simulation. Body weights for other days in the year were calculated by a finite difference method as: $BW_{(t)} = BW_{(t-1)} + GC_{YI} \times T$; where GC_{YI} is the temperature-dependent growth constant for a given year interval and T is the water temperature (°C). The GC_{YI} was iteratively fit for each year class so that the predicted body weight of fish at the next May 20th date corresponded to the body weight predicted under the constant temperature scenario. The fitted coefficients for each year class are described in the footnotes of Table 4.

Whole body lipid contents (g lipid per g body weight) were predicted from the temperature-dependent algorithm used for medium and large yellow perch described in Drouillard et al. (2009). For the constant temperature simulations, all fish had a constant fractional lipid content of 0.086 (by weight). For the dynamic temperature scenario, lipid content ratios varied between 0.043 and 0.093, depending on the temperature. Water content of the fish was predicted from the negative correlation between %moisture and %lipid as described in Drouillard et al. (2009). The lean dry

Table 4 Model parameters and variables used in yellow perch non-steady state bioaccumulation simulations

Model parameter/variable	Constant temperature simulation	Variable temperature simulation
Chemical log K_{OW}	6.5	6.5
C_w—Concentration in water (ng/mL)	0.001	0.001
C_{food}—Concentration in food (ng/g ww)[a]	79.85	79.85
$f_{LEQ(food)}$—Lipid equivalent content of food	0.025	0.025
$f_{L(food)}$—Lipid content of food	0.015	0.015
$f_{LDP(food)}$—Lead dry protein content of food	0.205	0.205
E_D—Energy density of food (kJ/g)	4.28	4.28
E_{diet}—Energy assimilation from diet	0.644	0.644
E_{food}—Digestion efficiency of food[b]	0.863	0.863
$C_{fish(0)}$—Initial concentration in fish (ng/g ww)[c]	305.07	269.02
$f_{LEQ(EX)}$—Lipid equivalent content of feces	0.0053	0.0053
T—Temperature (°C)	21	Variable[d]
L—Body length of fish (cm)[e]	Variable with age	NA
BW—Body weight of fish (g)[f,g]	$BW = 10^{(\log (L) \times 3.267 - 2.30)}$	Temperature dependent growth[g]
$f_{L(fish)}$—Lipid content of fish[h]	0.0863	Temperature dependent
$f_{w(fish)}$—Water content of fish[i]	$f_{w(fish)} = -0.68 \times f_{L(fish)} + 76.9$	$-0.68 \times f_{L(fish)} + 76.9$
$f_{LDP(fish)}$—Lean dry protein content of fish	$f_{LDP(fish)} = 1 - f_{w(fish)} - f_{L(fish)}$	$f_{LDP(fish)} = 1 - f_{w(fish)} - f_{L(fish)}$
$f_{LEQ(fish)}$—Lipid equivalents content of fish	$f_{LEQ(fish)} = f_{L(fish)} + 0.05 f_{LDP(fish)}$	$f_{LEQ(fish)} = f_{L(fish)} + 0.05 f_{LDP(fish)}$
ΔX_L—Daily lipid growth increment (g)	$\Delta X_L = X_{L(t)} - X_{L(t-1)}$	$\Delta X_L = X_{L(t)} - X_{L(t-1)}$
ΔX_{LDP}—Daily protein growth increment (g)	$\Delta X_{LDP} = X_{LDP(t)} - X_{LDP(t-1)}$	$\Delta X_{LDP} = X_{LDP(t)} - X_{LDP(t-1)}$
ΔG_L—Energy cost of lipid growth (kJ/d)	$\Delta G_L = \Delta X_L$ 39.3 always positive or 0	$\Delta G_L = \Delta X_L \times 39.3$ term may be positive or negative for weight gain or weight loss
ΔG_P—Energy cost of protein growth (kJ/d)	$\Delta G_P = \Delta X_L \times 18$ always positive or 0	$\Delta G_P = \Delta X_L \times 18$ term may be positive or negative due to weight gain or weight loss
D_{O2}—Oxycalorific coefficient (kJ/g O_2)	14.3	14.3
SMR × A—Standard metabolic rate and activity cost multiplier (kJ/g BW/d)[j]	$SMR \times A = 0.01 \times BW^{0.72} \times e^{(0.19 \times T)} \times 0.024 \times D_{O2} \times 1.5/BW$	$SMR \times A = 0.01 \times BW^{0.72} \times e^{(0.19 \times T)} \times 0.024 \times D_{O2} \times 1.5/BW$
SDA—Specific dynamic action (kJ/g BW/d)[j]	$SDA = 0.172 \times (SMR \times A + \lvert \Delta G_L \rvert + \lvert \Delta GP \rvert)$	$SDA = 0.172 \times (SMR \times A + \lvert \Delta G_L \rvert + \lvert \Delta GP \rvert)$
U—Excretion (kJ/g BW/d)[j]	$U = 0.0253 \times T^{0.58} \times e^{-0.299} \times (SMR \times A + \lvert \Delta G_L \rvert + \lvert \Delta GP \rvert)$	$U = 0.0253 \times T^{0.58} \times e^{-0.299} \times (SMR \times A + \lvert \Delta G_L \rvert + \lvert \Delta GP \rvert)$

Q_{feed}—Food consumption (kJ/g BW/d)	$Q_{feed} = \pm\Delta G_L \pm \Delta G_P + SMR \times A + SDA + U$	$Q_{feed} = \pm\Delta G_L \pm \Delta G_P + SMR \times A + SDA + U$
R—Respiration (kJ/g/BW/d)[j]	$R = SMR \times A + SDA \times U$	$R = SMR \times A + SDA \times U$
C_{O2}–Dissolved oxygen concentration in water (g/mL)[j]	$14.45–0.413 \times T + 5.56 \times 10^{-3} \times T^2/1 \times 10^{-6}$	$14.45–0.413 \times T + 5.56 \times 10^{-3} \times T^2/1 \times 10^{-6}$
E_{O2}—Oxygen efficiency across gills	0.6	0.6
G_v—Gill ventilation (mL/g/d)	$G_v = R/(D_{O2} \times C_{O2} \times E_{O2})$	$G_v = R/(D_{O2} \times C_{O2} \times E_{O2})$
G_{feed}—Food ingestion rate (g/g/d)	$G_{feed} = Q_{feed}/E_D$	$G_{feed} = Q_{feed}/E_D$
G_{ex}—feces excretion rate (g/g/d)	$G_{ex} = G_{feed} \times E_{food}$	$G_{ex} = G_{feed} \times E_{food}$
K_{BW}—Biota/water partition coefficient	$K_{BW} = K_{OW} \times f_{LEQ(fish)}$	$K_{BW} = K_{OW} \times f_{LEQ(fish)}$
K_{BEX}—Biota/feces partition coefficient	$K_{BEX} = f_{LEQ(EX)}/f_{LEQ(fish)}$	$K_{BEX} = f_{LEQ(EX)}/f_{LEQ(fish)}$
AE_w—Chemical extraction efficiency across gills	0.54	0.54
AE_{food}—Dietary chemical assimilation efficiency	0.6	0.6
IN_{Wat}—Daily chemical intake from water (ng/d)	$IN_{Wat} = G_v \times C_w \times AE_w \times BW$	$IN_{Wat} = G_v \times C_w \times AE_w \times BW$
IN_{food}—Daily chemical intake from food (ng/d)	$IN_{food} = G_{feed} \times C_{food} \times AE_f \times BW$	$IN_{food} = G_{feed} \times C_{food} \times AE_f \times BW$
OUT_{wat}—Daily loss chemical to water (ng/d)	$OUT_{Wat} = G_v \times AE_w \times BW \times C_{fish(t-1)}/K_{BW}$	$OUT_{Wat} = G_v \times AE_w \times BW \times C_{fish(t-1)}/K_{BW}$
OUT_{EX}—Daily loss of chemical to feces (ng/d)	$OUT_{EX} = G_{ex} \times AE_{food} \times BW \times C_{fish(t-1)}/K_{BW}$	$OUT_{EX} = G_{ex} \times AE_{food} \times BW \times C_{fish(t-1)}/K_{BW}$
$X_{fish(t)}$—Mass of chemical in fish at time t (ng)	$X_{fish(t)} = X_{fish(t-1)} + IN_{Wat} + IN_{food} - OUT_{Wat} - OUT_{EX}$	$X_{fish(t)} = X_{fish(t-1)} + IN_{Wat} + IN_{food} - OUT_{Wat} - OUT_{EX}$
$C_{(t)}$—Concentration in fish at time t (ng/g lipid equivalents)	$C_{(t)} = X_{fish(t)}/(BW \times f_{LEQ(fish)})$	$C_{(t)} = X_{fish(t)}/(BW \times f_{LEQ(fish)})$

[a]Food was assumed to be in equilibrium with water. $C_{food} = K_{OW} \times C_w \times f_{LEQ}$, where C_W is the concentration of chemical in water and f_{LEQ} is the lipid equivalent fraction in food

[b]Digestion efficiency of food refers to the reduction in volume of feces per unit of food consumed. Estimation based on a lipid assimilation efficiency of 0.92, lean dry protein assimilation efficiency of 0.6, and water assimilation of 0

[c]Year 1 fish on day 364 were assumed to be in equilibrium with water. $C_{fish(o)} = K_{OW} \times C_w \times f_{LEQ}$, where C_W is the concentration of chemical in water and f_{LEQ} is the lipid equivalent fraction in food

[d]Variable temperature involved a repeating temperature cycle measured in mesocosm tanks in Windsor, Ontario as described in (Drouillard et al. 2009). Day 1 of the simulation corresponded to May, 20 with a temperature of 16.0 °C

[e]Von Bertalanffy Growth curve for yellow perch reported by (Jackson et al. 2008). Total Length (cm) = $[280.5 \times (1 - e(-0.332 \times (Age + 0.031))]/10$, where Age is in days

[f]Body weight versus length relationship was based on seasonally collected yellow perch from ponds in southwestern Ontario (Unpublished data)

[g]Growth rates were fitted to be temperature dependent. For each birthday of the fish (May 20, years 1–8), the body weight was set to the body weight used for the constant temperature simulation. A temperature and year dependent growth constant (GC_{YI}) was fitted for each year interval to achieve the target body weight by the next anniversary. The equation was: $BW = GC_{YI} \times T + BW_{(t-1)}$, where GC is specific to each year class (0.0046; 0.0074; 0.0083; 0.0079; 0.0067; 0.0054; 0.0043; and 0.003 for years 1–2, 2–3, 3–4, 4–5, 5–6, 6–7, 7–8, and 8+) and T is the water temperature (°C)

[h]Calculated using a temperature-dependent algorithm reported for medium and large yellow perch by (Drouillard et al. 2009). % Lipid = $0.23 \times T + 3.8$. f_{lipid} = % Lipid/100

[i]Relationship between moisture content of yellow perch and lipid content of yellow perch reported by (Drouillard et al. 2009)

[j]Based on yellow perch algorithms for SMR, SDA and U reported by (Drouillard et al. 2009)

weight of fish was subsequently estimated by subtracting the water and lipid weights from the fish body weight. Daily changes in whole body lipid and lean dry weights were used to estimate growth increments, growth energy costs and lipid equivalent contents for each time step (see Table 4 for details). Daily estimates of food consumption rates (g food consumed per g body weight per day) and gill ventilation rates (mL water ventilated per g body weight per day) for yellow perch were calculated from temperature and size dependent algorithms as described in Drouillard et al. (2009) and detailed in Table 4.

The uptake portion of the toxicokinetics sub-model used the calculation methods of Arnot and Gobas (2004). Uptake flux of chemical into fish from water (ng/d) was estimated as the product of gill ventilation rate (mL per g body weight per day), chemical extraction efficiency across gills (unitless), chemical concentration in water (ng per mL), and body weight (g) of fish. In both scenarios, the recommended value of 0.54 was used for the chemical extraction efficiency across gills. The uptake flux of chemical into fish from food (ng/d) was estimated as the product of the feeding rate, dietary assimilation efficiency of the chemical, chemical concentration in food and body weight of fish. A constant value of 0.6 was used as the dietary assimilation efficiency value of the chemical. Chemical loss from fish (ng/d) via gills and feces were estimated as detailed in Drouillard et al. (2009), and described in Table 4. For simplicity of the simulations, the same chemical extraction efficiency across gills was used as the uptake algorithm. Similarly, the organism/feces chemical exchange efficiency was set to be equal to the dietary chemical assimilation efficiency described above.

Yellow perch model simulations were performed to predict bioaccumulation and bioamplification of a negligibly metabolized POP compound having a log K_{OW} of 6.5. Two different simulation scenarios were established to compare bioamplification under an artificial baseline condition of constant temperatures and a seasonally dynamic scenario that is consistent with temperate aquatic ecosystems. The baseline scenario involved a simulation, in which temperature was kept constant (21 °C; at the species optimum) across seasons and years. The seasonal scenario involved a simulation, in which an annual temperature profile that is consistent with measurements made in aquaculture ponds of Southern Ontario, was applied to predict the seasonal variation in lipid content and its impact on chemical bioamplification. The same annual temperature profile was cycled across simulation years. In both simulations, the model was initialized by assuming Age 1 fish were in chemical equilibrium with water. Fish were assumed to feed on a stable food source (constant in its proximate composition, energy density and chemical concentrations) over the duration of the simulation. The concentration of chemical in food was set so that the food was in equilibrium with the concentration of chemical in water.

The yellow perch non-steady state bioaccumulation model was developed using a Microsoft Excel spreadsheet. The model is a finite difference model run at a daily time steps for 2,920 days. The model was initialized with a temperature of 15.9 °C and fish aged 365 d (May 20, year 1), body weight of 4.84 g, lipid content of 7.5%, moisture content of 71.8%. The initial fish concentration was set to be in equilibrium with water. Food concentration was set to be in equilibrium with water. The food concentration we held constant throughout the experimental duration.

11 Appendix 2: Description of the Herring Gull Model and Associated Simulations

The herring gull bioenergetic and toxicokinetics model is described in several papers (Norstrom et al. 1986a, b, 2007; Clark et al. 1987, 1988; Drouillard et al. 2003). Most commonly, the model has been used to describe non-steady bioaccumulation of POPs in adult female life stages over multi-year periods. However, the basic algorithms for chick growth and bioenergetics of early and late life stages for both sexes are detailed in Norstrom et al. (1986b). For simplicity, the herring gull model simulations were formulated for male birds to circumvent the need to consider chemical depuration by egg laying, and to maximize predictions of bioamplification in the species. The model was expanded to include three linked life-stages: a chick stage (post-pipping to fledging), immature adult (post fledging to 3.8 years), and a reproductive adult (3.8 years to 8 years) stage. The chick stage immediately experiences bioamplification from maternally deposited residues (Drouillard et al. 2003), followed by growth dilution until fledging. The subadult male experiences seasonal temperature variation and proximate composition, but does not participate in reproductive activities (such as courtship, or the feeding and foraging costs associated with rearing a clutch of chicks). Adult males experience additional foraging costs associated with the later activities. Although herring gulls have much longer life spans than the 8-year period of the model simulation, an 8-year duration was selected for consistency with yellow perch simulations.

For each life stage, the bioenergetic sub-model predicts growth, proximate composition, and food consumption as outlined in Norstrom et al. (1986a). The toxicokinetics model only considers chemical uptake from food, since air uptake by birds is negligible (Drouillard et al. 2012). Similar to the yellow perch model, the uptake flux of chemical into the bird from food (ng/d) was estimated as the product of the feeding rate, dietary assimilation efficiency of chemical, chemical concentration in food, and body weight of fish. A constant value of 0.9 was used as the dietary assimilation efficiency value for the chemical and was derived from data collected for ring doves (Drouillard and Norstrom 2000). The toxicokinetic parameters necessary to describe chemical elimination included the plasma/fat partition coefficient (K_{PF}) and plasma clearance coefficient (k'_{pc}). For model simulations, the values of K_{PF} and k'_{pc} for mirex, measured in juvenile herring gulls (Clark et al. 1987), were used and were assumed to be constant across the different life stages. Mirex was chosen to represent a highly hydrophobic POP that is negligibly biotransformed in birds. A modification to the herring gull model not applied in previous publications of the model was that the chemical outflux was measured by multiplying the k'_{pc} by the body weight and lipid equivalent concentration of chemical in the animal tissues. Past iterations of the module used the lipid normalized concentration. This change was made to make the model more consistent with the yellow perch model. However, it should be noted that the fish and bird models differ fundamentally in how elimination flux is treated. In the herring gull model, k'_{PC} is a constant, and elimination flux varies over the year only as a result of changes in the proximate

composition (lipid equivalent content) of the animal. In the fish model, elimination flux of the chemical depends on variation in proximate composition, as well as variation in gill ventilation and feeding rates. These differences result in a decoupling of feeding rates and chemical elimination in birds that causes lags in return to steady state, following sudden shifts in feeding rates. This is exemplified in Fig. 2c for the constant temperature, post-adult male simulation. No attempts were made to harmonize the two model organisms into a single toxicokinetic model, because we preferred to preserve the characteristics and attributes of the models that had been addressed in their original publications.

As for the yellow perch models, two simulation scenarios were established for herring gulls. The baseline simulation kept temperature and photoperiod constant at 21 °C and 12 h/d across seasons and years. The seasonal scenario used temperature and photoperiod data from Lake Ontario that had been collected during 1997. The model used monthly mean temperature and photoperiod data and interpolated temperature and photoperiods for each day of the simulation. The model cycled the same annual temperature profile across all years in each simulation. The model was initialized using a fresh egg concentration predicted from a 10-year adult female model simulation (Clark et al. 1988), wherein the female bird was fed a constant diet of the same concentration and energy density as that used for male simulations. The female simulation used a constant temperature and photoperiod to initialize the constant temperature simulation, and a variable temperature and photoperiod equivalent to the Lake Ontario profile to initialize the dynamic temperature simulation. The simulated fresh egg concentration (μg/kg wet weight) from adult female simulations was multiplied by the egg weight (85 g), and was divided by the fresh egg lipid content (7.2 g) as reported by Drouillard et al. (2003) to estimate the lipid normalized egg concentration. Bioamplification of fresh egg residues in the pipping embryo was accounted for by multiplying the fresh egg lipid normalized concentration by a factor of 3.1 (Drouillard et al. 2003), and multiplied by the lipid equivalent content of the newly pipped chick to determine the total mass of chemical in the chick. The bird was grown out and was assumed to feed on a constant food source of proximate composition, energy density, and chemical concentration that was similar for the duration of the study. A full description of model parameters and algorithms employed is presented in Table 5.

The herring gull toxicokinetic model output was copied onto a Microsoft Excel spreadsheet. The model is a finite difference model and was run at a daily time steps for 3,137 days. The model was initialized with a 1-day-old pipping male chick hatched on May 29, 1997. The chick sub-model was used to calculate growth, proximate composition, bioenergetics, and chemical toxicokinetics between days 1 and 88. The output from the chick sub-model was linked to a subadult male model between days 89 and 1,398, i.e., up to 4 years. In the subadult model, immature birds were assumed to not participate in reproductive activities and therefore had no courtship feeding or chick provisioning costs. The output from the subadult male model was linked to a reproductive adult male model which covered simulation days 1,399–3,136.

Table 5 Model parameters and variables used in herring gull non-steady state bioaccumulation simulations

Model parameter/variable	Constant temperature simulation	Variable temperature simulation
Parameters common to chick and adult sub-models		
K_{pf}—Plasma/fat distribution coefficient[a]	0.0067	0.0067
k'_{pc}—Plasma clearance coefficient (L/kg/d)[a]	0.041	0.041
C_{food}—Concentration in food (ng/g ww)	79.85	79.85
E_D—Energy density of food (kcal/g)	1.24	1.24
E_{diet}—Energy assimilation from diet[b]	0.85	0.85
AE_{food}—Dietary chemical assimilation efficiency[c]	0.9	0.9
T—Temperature (°C)[d]	21	Variable by season
PP—Photoperiod (h daylight/d)[d]	12	Variable by season
Chick sub-model (days 1–88)		
$C_{chick(0)}$—Initial concentration in pipping chick (ng/g lipid weight)[e]	54,012	101,243
BW—Time dependent body weight of chick[f]	$BW = 1{,}193 \times \exp^{[-\exp(-0.075\times(Age-16.3))]}$	$BW = 1{,}193 \times \exp^{[-\exp(-0.075\times(Age-16.3))]}$
I_w—Water content of chick per g of lean dry weight (g/g)[g]	$I_W = 4.255–0.061$ age (days 3–36). See footnote	$I_W = 4.255–0.061$ age (days 3–36). See footnote
I_L—Lipid content of chick per g of lean dry weight (g/g)[b]	0.24	0.24
LDW—Lean dry weight of chick (g)	$LDW = BW/(1 + I_W + I_L)$	$LDW = BW/(1 + I_W + I_L)$
X_{lipid}—Mass of lipid in chick (g)	$X_{lipid} = LDW \times I_L$	$X_{lipid} = LDW \times I_L$
X_{LEQ}—Mass of lipid equivalents in chick (g)	$X_{LEQ} = X_{lipid} + 0.05 \times LDW$	$X_{LEQ} = X_{lipid} + 0.05 \times LDW$
$Q_{feed(chick)}$—Food consumption rate of chick (kcal/d)[h]	Estimated on a daily basis Days 1–88. See footnote for details	Estimated on a daily basis Days 1–88. See footnote for details
G_{feed}—Food ingestion rate (g/g/d)	$G_{food} = Q_{feed(chick)}/E_D$	$Q_{food} = Q_{feed(chick)}/E_D$
IN_{food}—Daily chemical intake from food (ng/d)	$IN_{food} = G_{feed} \times C_{food} \times AE_{food}$	$IN_{food} = G_{feed} \times C_{food} \times AE_{food}$
OUT_{EX}—Daily loss of chemical (ng/d)	$OUT_{EX} = k'_{pc} \times BW \times C_{(t-1)} \times K_{pf}$	$OUT_{EX} = k'_{pc} \times BW \times C_{(t-1)} \times K_{pf}$
$X_{chick(t)}$—Mass of chemical in chick at time t (ng)	$X_{chick(t)} = X_{chick(t-1)} + IN_{food} - OUT_{EX}$	$X_{chick(t)} = X_{chick(t-1)} + IN_{food} - OUT_{EX}$
$C_{(t)}$—Concentration of chemical in chick at time t (ng/g lipid weight)	$C_{(t)} = X_{chick(t)}/X_{LEQ}$	$C_{(t)} = X_{chick(t)}/X_{LEQ}$
Immature male sub-model (days 89–1,397)		
f_{lipid}—Fraction of lipid in body[b]	0.079	$f_{lipid} = (-0.27 \times T + 3.4)/100$

(continued)

Table 5 (continued)

Model parameter/variable	Constant temperature simulation	Variable temperature simulation
LDW—Lean dry weight of male (g)[b]	314	314
BW—Body weight of male (g)	1,098	$BW = LDW \times 3.22/(1-f_{lipid})$
X_{lipid}—Lipid weight of male (g)	86.97	$X_{lipid} = BW \times f_{lipid}$
X_{LEQ}—Lipid equivalent weight of male (g)	102.67	$X_{LEQ} = X_{lipid} + 0.05 \times LDW$
ΔX_L—daily growth increment of lipid (g)	0	$\Delta X_{lipid} = X_{lipid(t)} - X_{lipid(t-1)}$
MR—Metabolic rate due to basal metabolism and thermoregulation (kcal/d)	141.6	$SMR = (3.35 + 0.05PP) \times BW^{0.544} - ((0.141 + 0.006PP) \times BW^{0.3})T$
ΔG_L Energy cost of lipid growth (kJ/d)	0	$\Delta G_L = \Delta X_L \times 9.4$ Term may be positive or negative due to weight gain or weight loss
F—Foraging costs (kcal/d)[i]	55.1	$F = (0.28/(1-0.28)) \times (MR \pm \Delta G_L)$
Q_{feed}—Food consumption rate of subadult male (kcal/d)	$Q_{feed} = MR + F$	$Q_{feed} = \pm \Delta G_L + MR + F$
G_{feed}—Food ingestion rate (g/g/d)	$G_{feed} = Q_{feed}/E_D$	$G_{feed} = Q_{feed}/E_D$
IN_{food}—Daily chemical intake from food (ng/d)	$IN_{food} = G_{feed} \times C_{food} \times AE_{food}$	$IN_{food} = G_{feed} \times C_{food} \times AE_{food}$
OUT_{EX}—Daily loss of chemical (ng/d)	$OUT_{EX} = k'_{pc} \times BW \times C_{(t-1)} \times K_{pf}$	$OUT_{EX} = k'_{pc} \times BW \times C_{(t-1)} \times K_{pf}$
$X_{subadult(t)}$—Mass of chemical in subadult male at time t (ng)	$X_{subadult(t)} = X_{subadult(t-1)} + IN_{food} - OUT_{EX}$	$X_{subadult(t)} = X_{subadult(t-1)} + IN_{food} - OUT_{EX}$
$C_{(t)}$—Concentration at time t (ng/g lipid equivalents weight)	$C_{(t)} = X_{suzbadult(t)}/X_{LEQ}$	$C_{(t)} = X_{subadult(t)}/X_{LEQ}$
Mature male sub-model (days 1,398–3,137)		
f_{lipid}—Fraction of lipid in adult tissues[b]	0.079	$f_{lipid} = (-0.27 \times T + 13.4)/100$
LDW—Lean dry weight of adult male (g)[b]	314	314
BW—Body weight of adult male (g)	1,098	$BW = LDW \times 3.22/(1-f_{lipid})$
X_{lipid}—Lipid weight of adult male (g)	86.97	$X_{lipid} = BW \times f_{lipid}$
X_{LEQ}—Lipid equivalent weight of male (g)	102.67	$X_{LEQ} = X_{lipid} + 0.05 \times LDW$
ΔX_L—Daily growth increment of lipid (g)	0	$\Delta X_L = X_{lipid(t)} - X_{lipid(t-1)}$
MR—Metabolic rate due to basal metabolism and thermoregulation costs (kcal/d)	141.6	$SMR = (3.35 + 0.05PP) \times BW^{0.544} - ((0.141 + 0.006PP) \times BW^{0.3})T$
ΔG_L Energy cost of lipid growth (kJ/d)	0	$\Delta G_L = \Delta X_L \times 9.4$ Term may be positive or negative due to weight gain or weight loss
F—Foraging costs (kcal/d)[i]	55.1	$F = (0.28/(1-0.28)) \times (MR \pm \Delta G_L)$

CF—Courtship feeding costs (kcal/d)[j]	Estimated on a daily basis for days March 27–April 25 during years 4–8 of the simulation. See footnote	Estimated on a daily basis for days March 27–April 25 during years 4–8 of the simulation. See footnote
CR—Chick rearing costs (kcal/d)[k]	Estimated on daily basis for days May 28–Aug 24 during years 4–8 of the simulation. See footnote	Estimated on daily basis for days May 28–Aug 24 during years 4–8 of the simulation. See footnote
	$CR = [0.28/(1-0.28) \times (Q_{feed(chick)})] \times N_{chicks}/2$	$CR = [0.28/(1-0.28) \times (Q_{feed(chick)})] \times N_{chicks}/2$
Q_{feed}—Food consumption rate of subadult male (kcal/d)	$Q_{feed} = MR + F + CF + CR$	$Q_{feed} = \pm \Delta G_L + MR + F + CF + CR$
G_{feed}—Food ingestion rate (g/g/d)	$G_{feed} = Q_{feed}/E_D$	$G_{feed} = Q_{feed}/E_D$
IN_{food}—Daily chemical intake from food (ng/d)	$IN_{food} = G_{feed} \times C_{food} \times AE_{food}$	$IN_{food} = G_{feed} \times C_{food} \times AE_{food}$
OUT_{EX}—Daily loss of chemical (ng/d)	$OUT_{EX} = k'_{pc} \times BW \times C_{(t-1)} \times K_{pf}$	$OUT_{EX} = k'_{pc} \times BW \times C_{(t-1)} \times K_{pf}$
$X_{adult(t)}$—Mass of chemical in subadult male at time t (ng)	$X_{adult(t)} = X_{adult(\tau-1)} + IN_{food} - OUT_{EX}$	$X_{adult(t)} = X_{adult(t-1)} + IN_{food} - OUT_{EX}$
$C_{(t)}$—Concentration at time t (ng/g lipid equivalents weight)	$C_{(t)} = X_{adult(t)}/X_{LEQ}$	$C_{(t)} = X_{adult(t)}/X_{LEQ}$

[a]Equivalent value for herring gulls as reported for mirex in (Clark et al. 1987)

[b]Estimate for herring gulls as reported in (Norstrom et al. 1986a, b)

[c]Reported dietary assimilation efficiency of PCBs in ring doves from Drouillard and Norstrom (2000)

[d]Average monthly values of temperature and photoperiod for Lake Ontario during 1997 were used as recommended for the default model inputs in the visual basic version of the Herring gull model. The same monthly means were repeated across the different years of the simulation

[e]The herring gull visual basic model was run for an adult female with an initial bird concentration of zero; birds were fed a constant diet containing 79.85 ng/g of chemical for 8 years until steady state was achieved. The model predicted egg concentration after 8 years was 2,763 ng/g wet weight. The fresh egg concentration was converted to a lipid normalized egg concentration of 32,619 ng/g lipid weight using a fresh egg weight of 85 g and egg lipid content of 7.2 g (Drouillard et al. 2003). The fresh egg concentration was multiplied by 3.1 to account for bioamplification in the embryo as reported for herring gull chicks at the time of pipping (Drouillard et al. 2003)

[f]Male chick Gompertz growth equation reported by (Norstrom et al. 1986a, b). Chick age is in days. Growth curve used until day 58 when predicted chick weight became equivalent to adult male weight

[g]The water content per lean dry weight content was set to 2.81 and 3.84 for day 1 and 2. Between days 3 and 36, it was estimated according to $I_W = 4.255–0.061$ age (days 3–36) as reported in (Norstrom et al. 1986a, b). The parameter was then held constant at a value of 2 for days 37–89. Beyond day 89, the subadult model was used and does not require this parameter

[h]Based on total energy intake per chick per day for herring gull chicks extrapolated from Fig. 2 of Norstrom et al. (1986a, b) between days 1 and 70. Between days 71 and 89, value held constant at the adult sub-model start value of 232.6 kcal/d

[i]Foraging coefficient established at 0.28 as recommended for Great Lakes herring gulls by Norstrom et al. (1986a, b). Constant of 9.4 represents the energy per gram of fat (kcal/g)

[j]Courtship feeding costs were interpolated on a daily basis from data presented in Table 5 of Norstrom et al. (1986a, b)

[k]Chick rearing costs consider the additional foraging cost associated with feeding a clutch of chicks (kcal/d). Daily energy requirements of chicks are established in footnote h. The foraging cost increment for the adult male is given by: $CR = [(0.28/(1-0.28)) \times (C_{chick})] \times N_{chicks}/2$, where C_{chick} is the daily energy intake of each chick (kcal/d), 0.28 is the foraging coefficient (see footnote i) and N_{chick} is the number of chicks (3) reared each year. The function is divided by 2 because it is assumed that adult male birds contribute to 50% of the food provisioning for a clutch of chicks

References

Addison RF, Stobo WT (1993) Organochlorine concentrations and burdens in grey seal (*Halichoerus grypus*) blubber during the first year of life. J Zool Lond 230:443–450

Alonso E, Tapie N, Budzinski H, Leménach K, Peluhet L, Tarazona JV (2008) A model for estimating the potential biomagnification of chemicals in a generic food web: preliminary development. Env Sci Pollut Res 15:31–40

Angell RA, Haffner GD (2010) Polychlorinated biphenyl elimination rates and changes in chemical activity in hibernating amphibians. Environ Toxicol Chem 29:700–707

Arnot JA, Gobas FAPC (2003) A generic QSAR for assessing the bioaccumulation potential of organic chemicals in aquatic food webs. QSAR Comb Sci 22:337–345

Arnot JA, Gobas FAPC (2004) A food web bioaccumulation model for organic chemicals in aquatic ecosystems. Environ Toxicol Chem 23:2343–2355

Arnot JA, Gobas FA (2006) A review of bioconcentration factor (BCF) and bioaccumulation factor (BAF) assessments for organic chemicals in aquatic organisms. Environ Rev 14:257–297

Antunes P, Gil O, Ferreira M, Vale C, Reis-Henriques MA (2007) Depuration of PCBs and DDTs in mullet under captivity clean conditions. Chemosphere 57:58–64

Barber MC, Suarez LA, Lassiter RR (1988) Modeling bioconcentration of nonpolar organic pollutants by fish. Environ Toxicol Chem 7:545–558

Barber MC (2003) A review and comparison of models for predicting dynamic chemical bioconcentration in fish. Environ Toxicol Chem 22:1963–1992

Barber MC (2008) Dietary uptake models used for modeling the bioaccumulation of organic contaminants in fish. Environ Toxicol Chem 27:755–777

Barron MG (1990) Bioconcentration. Will water-borne organic chemicals accumulate in aquatic animals? Environ Sci Technol 24:1612–1618

Bartrons M, Grimalt JO, Catalan J (2007) Concentration changes of organochlorine compounds and polybromodiphenyl ethers during metamorphosis of aquatic insects. Environ Sci Technol 41:6137–6141

Beacham TD, Murray CB, Withler RE (1989) Age, morphology, and biochemical genetic variation of Yukon river chinook salmon. Trans Am Fish Soc 118:46–63

Belpaire C, Goemans G (2007) Eels: contaminant cocktails pinpointing environmental contamination. ICES J Mar Sci 64:1423–1436

Bhavsar SP, Gewurtz SB, McGoldrick DJ, Keir MJ, Backus SM (2010) Changes in mercury levels in Great Lakes fish between 1970s and 2007. Environ Sci Technol 44:3273–3279

Black MC, McCarthy JF (1988) Dissolved organic macromolecules reduce the uptake of hydrophobic organic contaminants by the gills of rainbow trout (*Salmo gairdneri*). Environ Toxicol Chem 7:593–600

Blais JM, Wilhelm F, Kidd KA, Muir DCG, Donald DB, Schindler DW (2003) Concentrations of organochlorine pesticides and polychlorinated biphenyls in amphipods (*Gammarus lacustris*) along an elevation gradient in mountain lakes of western Canada. Environ Toxicol Chem 22:2605–2613

Bligh EG, Dyer WJ (1959) A rapid method of total lipid extraction and purification. Can J Biochem Physiol 37:911–917

Boon JP, Duinker JC (1985) Kinetics of polychlorinated biphenyl (PCB) components in juvenile sole (*Solea solea*) in relation to concentrations in water and to lipid metabolism under conditions of starvation. Aquat Toxicol 7:119–134

Boon JP, Eijgenraam F, Everaarts JM, Duinker JC (1989) A structure-activity relationship (SAR) approach towards metabolism of PCBs in marine animals from different trophic levels. Mar Environ Res 27:159–176

Boon JP, Oostingh I, van der Meer J, Hillebrand TJ (1994) A model for the bioaccumulation of chlorobiphenyl congeners in marine mammals. Eur J Pharmacol 270:237–251

Borgå K, Fisk AT, Hoekstra PF, Muir DCG (2004) Biological and chemical factors of importance in the bioaccumulation and trophic transfer of persistent organochlorine contaminants in Arctic marine food webs. Environ Toxicol Chem 23:2367–2385

Borgå K, Kidd KA, Muir DCG, Berglund O, Conder JM, Gobas FAPC, Kucklick J, Malm O, Powell DE (2012) Trophic magnification factors: considerations of ecology, ecosystems and study design. Int Environ Assess Manage 8:64–84

Braune BM, Norstrom RJ (1989) Dynamics of organochlorine compounds in herring gulls: 3 tissue distribution and bioaccumulation in Lake Ontario gulls. Environ Toxicol Chem 8:957–968

Bull CD, Metcalfe NB, Mangel M (1996) Seasonal matching of foraging to anticipated energy requirements in anorexic juvenile salmon. Proc R Soc London Ser B 263:13–18

Bustnes JO, Moe B, Herzke D, Hanssen SA, Nordstad T, Sagerup K, Gabrielsen GW, Borgå K (2010) Strongly increasing blood concentrations of lipid-soluble organochlorines in high arctic common eiders during incubation fast. Chemosphere 79:320–325

Bustnes JO, Moe B, Hanssen AA, Herzke D, Fenstad AA, Nordstad T, Borga K, Gabrielsen GW (2012) Temporal dynamics of circulating persistent organic pollutants in a fasting seasbird under different environmental conditions. Environ Sci Technol 46:10287–10294

Bystrom P, Andersson J, Kiessling A, Eriksson LO (2006) Size and temperature dependent foraging capacities and metabolism: consequences for winter starvation mortality in fish. Oikos 115:43–52

Campfens J, Mackay D (1997) Fugacity-based bodel of PCB bioaccumulation in complex aquatic food webs. Environ Sci Technol 31:577–583

Chevrier J, Dewailly E, Ayotte P, Despres JP, Tremblay A (2000) Body weight loss increase plasma and adipose tissue concentrations of potentially toxic pollutants in obese individuals. Int J Obese Related Metab Disord 24:1272–1278

Chiuchiolo AL, Dickhut RM, Cochran MA, Ducklow HW (2004) Persistent organic pollutants at the base of the Antarctic marine food web. Environ Sci Technol 38:3551–3557

Chou CC, Chen YN, Li CS (2004) Congener-specific polychlorinated biphenyls in cetaceans from Taiwan waters. Arch Environ Contam Toxicol 47:551–560

Chow BA, Hamilton J, Cattet MR, Stenhouse G, Obbard ME, Vijayan MM (2011) Serum corticosteroid binding globulin expression is modulated by fasting in polar bears (*Ursus maritimus*). Comp Biochem Physiol Part A Mol Integr Physiol 158:111–115

Christensen JR, MacDuffee M, Yunker MB, Ross P (2007) Hibernation-associated changes in persistent organic pollutant (POP) levels and patterns in British Columbia grizzly bears (*Ursus arctos horribilis*). Environ Sci Technol 41:1834–1840

Clark DR, Prouty RM (1977) Experimental feeding of DDE and PCB to female big brown bats (*Eptesicus fuscus*). J Toxicol Environ Health 2:917–928

Clark DR (1981) Bats and environmental contaminants: a review. U.S. Department of the Interior (Special Scientific Report # 235). Fish and Wildlife Service, Washington, DC, pp 1–29.

Clark DR Jr, Krynitsky AJ (1983) DDT: recent contamination in New Mexico and Arizona? Environment 25:27–31

Clark TP, Norstrom RJ, Fox GA, Won HT (1987) Dynamics of organochlorine compounds in herring gulls (*Larus argentatus*): II. A two-compartment model and data for ten compounds. Environ Toxicol Chem 6:547–559

Clark T, Clark K, Paterson S, Norstrom R, Mackay D (1988) Wildlife monitoring, modeling and fugacity. Environ Sci Technol 22:120–127

Clark KE, Gobas FAPC, Mackay D (1990) Model of organic chemical uptake and clearance by fish from food and water. Environ Sci Technol 24:1203–1213

Colabuono FI, Taniguchi S, Montone RC (2012) Organochlorine contaminants in albatrosses and petrels during migration in South Atlantic Ocean. Chemosphere 86:701–708

Connell DW (1988) Bioaccumulation behavior of persistent organic chemicals with aquatic organisms. Rev Environ Contam Toxicol 102:117–154

Connolly JP, Pedersen CJ (1988) A thermodynamic based evaluation of organic chemical accumulation in aquatic organisms. Environ Sci Technol 22:99–103

Cornelissen G, Gustafsson Ö, Bucheli TD, Jonker MTO, Koelmans AA, van Noort PCM (2005) Extensive sorption of organic compounds to black carbon, coal, and kerogen in sediments and soils: mechanisms and consequences for distribution, bioaccumulation, and biodegradation. Environ Sci Technol 39:6881–6895

Czub G, McLachlan MS (2004) A food chain model to predict the levels of lipophilic organic contaminants in humans. Environ Toxicol Chem 23:2356–2366

Czub G, McLachlan MS (2007) Influence of the temperature gradient in blubber of bioaccumulation of persistent lipophilic organic chemicals in seals. Environ Toxicol Chem 26:1600–1605

Dale WE, Gaines TB, Hayes WJ Jr (1962) Storage and excretion of DDT in starved rats. Toxicol App Pharmacol 4:89–106

Daley JM, Leadley TA, Drouillard KG (2009) Evidence for bioamplification of nine polychlorinated biphenyl (PCB) congeners in yellow perch (Perca flavescens) eggs during incubation. Chemosphere 75:1500–1505

Daley JM, Corkum LD, Drouillard KG (2011) Aquatic to terrestrial transfer of sediment associated persistent organic pollutants is enhanced by bioamplification processes. Environ Toxicol Chem 30:2167–2174

Daley JM, Leadley TA, Pitcher TE, Drouillard KG (2012) Bioamplification and the selective depletion of persistent organic pollutants in Chinook salmon larvae. Environ Sci Technol 46:2420–2426

DeBruyn AM, Gobas FAPC (2004) Modelling the diagenetic fate of persistent organic pollutants in organically enriched sediments. Ecol Model 179:405–416

DeBruyn AMH, Ikonomou MG, Gobas FAPC (2004) Magnification and toxicity of PCBs, PCDDs, and PCDFs in upriver migrating Pacific Salmon. Environ Sci Technol 38:6217–6224

DeBruyn AMH, Gobas FAPC (2006) A bioenergetic biomagnification model for the animal kingdom. Environ Sci Technol 40:1581–1587

DeBruyn AMH, Gobas FAPC (2007) The sorptive capacity of animal protein. Environ Toxicol Chem 26:1803–1808

Debier C, Pomeroy PP, Dupont C, Joiris C, Comblin V, Le Boulenge E, Larondelle Y, Thome JP (2003) Quantitative dynamics of PCB transfer from mother to pup during lactation in UK grey seals *Halicheorus grypus*. Mar Ecol Prog Ser 247:237–248

Debier C, Chalon C, Le Boeuf BJ, De Tillesse T, Larondelle Y, Thomé JP (2006) Mobilization of PCBs from blubber to blood in northern elephant seals (*Mirounga angustirostris*) during the post-weaning fast. Aquat Toxicol 80:149–157

DeFreitas AS, Norstrom RJ (1974) Turnover and metabolism of polychlorinated biphenyls in relation to their chemical structure and the movement of lipids in the pigeon. Can Physiol Pharm 52:1081–1094

Devillers J, Domine D, Bintein S, Karcher W (1998) Fish bioconcentration modeling with log P. Toxicol Mech Meth 8:1–10

Di Toro DM, Zarba CS, Hansen DJ, Berry WJ, Swartz RC, Cowan CE, Pavlou SP, Allen HE, Thomas NA, Paquin PR (1991) Technical basis for establishing sediment quality criteria for nonionic organic chemicals using equilibrium partitioning. Environ Toxicol Chem 10:1541–1583

Duursma EK, Nieuwenhuize J, Van Liere JM, de Rooy CM, Witte JIJ, Van der Meer J (1991) Possible loss of polychlorinated biphenyls from migrating European silver eels: a 3 month simulation experiment. Mar Chem 36:1–4

Drouillard KG, Norstrom RJ (2000) Dietary absorption efficiencies and toxicokinetics of polychlorinated biphenyls in ring doves following exposure to Aroclor mixtures. Environ Toxicol Chem 19:2707–2714

Drouillard KG, Fernie KJ, Smits JE, Bortolotti GR, Bird DM, Norstrom RJ (2001) Bioaccumulation and toxicokinetics of 42 polychlorinated biphenyl congeners in American kestrels (*Falco sparverius*). Environ Toxicol Chem 20:2514–2522

Drouillard KG, Norstrom RJ, Fox GA, Gilam A, Peakall DB (2003) Development and validation of a herring gull embryo toxicokinetic model for PCBs. Ecotoxicology 12:55–68

Drouillard KG, Hagen H, Haffner D (2004) Evaluation of chloroform/methanol and dichloromethane/hexane extractable lipids as surrogate measures of sample partition capacity for organochlorines in fish tissues. Chemosphere 55:395–400

Drouillard KG (2008) Biomagnification. In: Jorgensen SE, Fath BD (eds) Ecotoxicology vol 1 of encyclopedia of ecology, vol 5. Elsevier, Oxford, pp 441–448

Drouillard KG, Paterson G, Haffner D (2009) A combined food web toxicokinetic and species bioenergetic model for predicting seasonal PCB elimination in yellow perch (*Perca flavescens*). Environ Sci Technol 43:2858–2864

Drouillard KG, Paterson G, Liu J, Haffner GD (2012) Calibration of the gastrointestinal model to predict maximum biomagnification potentials of polychlorinated biphenyls in a bird and fish. Environ Sci Technol 46:10279–10286

Ecobichon DJ, Saschenbrecker PW (1969) The redistribution of stored DDT in cockerels under the influence of food deprivation. Toxicol Appl Pharmacol 15:420–432

Edmunds GF Jr, Jensen SL, Berner L (1976) The mayflies of North and Central America. University of Minnesota Press, Minneapolis, MN, USA

Elliott JE, Wilson LK, Langelier KW, Norstrom RJ (1996) Bald eagle mortality and chlorinated hydrocarbon contaminants in livers from British Columbia, Canada, 1989–1994. Environ Pollut 94:9–18

Escher BI, Ashauer R, Dyer S, Hermens JL, Lee JH, Leslie HA, Mayer P, Meador JP, Warne MS (2011) Crucial role of mechanisms and modes of toxic action for understanding tissue residue toxicity and internal effect concentrations of organic chemicals. Integr Environ Assess Manag 7:28–49

Ewald G, Larsson P, Linge H, Okla L, Szarzi N (1998) Biotransport of organic pollutants to an inland Alaska lake by migrating sockeye salmon (*Oncorhynchus nerka*). Arctic 51:40–47

Fenton MB, Barclay MR (1980) Myotis lucifugus. Mamm Sp 142:1–95

Fisk AT, Norstrom RJ, Cymbalisty CD, Muir DC (1998) Dietary accumulation and depuration of hydrophobic organochlorines: bioaccumulation parameters and their relationship with the octanol/water partition coefficient. Environ Toxicol Chem 17:951–961

Foekema EM, Fischer A, Parron ML, Kwadijk C, de Vries P, Murk AJ (2012) Toxic concentrations in fish early life stages peak at a critical moment. Environ Toxicol Chem 31:1381–1390

Fort J, Porter WP, Grémillet D (2009) Thermodynamic modelling predicts energetic bottleneck for seabirds wintering in the northwest Atlantic. J Exp Biol 212:2483–2490

Fuglei E, Øritsland NA (1999) Seasonal trends in body mass, food intake and resting metabolic rate, and induction of metabolic depression in arctic foxes (*Alopex lagopus*) at Svalbard. J Comp Physiol B 169:361–369

Fuglei E, Bustnes JO, Hop H, Mørk T, Björnfoth H, van Bavel B (2007) Environmental contaminants in arctic foxes (*Alopex lagopus*) in Svalbard: relationships with feeding ecology and body condition. Environ Pollut 146:128–138

Gabrielsen GW, Skaare JU, Polder A, Bakken V (1995) Chlorinated hydrocarbons in glaucous gulls (*Larus hyperboreus*) in the southern part of Svalbard. Sci Total Environ 160(161):337–346

Gewurtz SB, Backus SM, Bhavsar SP, McGoldrick DJ, de Solla SR, Murphy EW (2011) Contaminant biomonitoring programs in the Great Lakes region: review of approaches and critical factors. Environ Rev 19:162–184

Geyer H, Scheuntert I, Rapp K, Kettrup A, Korte F, Greim H, Rozman K (1990) Correlation between acute toxicity of 2,3,7,8-tetrachlorodibenzo-p-dioxin (TCDD) and total body fat content in mammals. Toxicology 95:97–107

Geyer HJ, Steinberg CE, Scheunert I, Brueggemann R, Schuetz W, Kettrup A, Rozman K (1993) A review of the relationship between acute toxicity (LC50) of gamma-hexachlorocyclohexane (gamma-HCH, lindane) and total lipid content of different fish species. Toxicology 83:169–179

Gobas FAPC, Opperhuisen A, Hutzinger O (1986) Bioconcetration of hydrophobic chemicals in fish: relationship with membrane permeation. Environ Toxicol Chem 5:637–646

Gobas FAPC, Muir DCG, Mackay D (1988) Dynamics of dietary bioaccumulation and faecal elimination of hydrophobic organic chemicals in fish. Chemosphere 17:943–962

Gobas FAPC (1993) A model for predicting the bioaccumulation of hydrophobic organic chemicals in aquatic food-webs: application to Lake Ontario. Ecol Model 69:1–17

Gobas FAPC, Zhang X, Wells R (1993) Gastrointestinal magnification: the mechanism of biomagnification and food chain accumulation of organic chemicals. Environ Sci Technol 27:2855–2863

Gobas FAPC, Wilcockson JB, Russell R, Haffner GD (1999) Mechanism of biomagnification in fish under laboratory and field conditions. Environ Sci Technol 33:133–141

Gobas FA, Morrison HA (2000) Bioconcentration and biomagnification in the aquatic environment. In: Boethling RS, Mackay D (eds) Handbook of property estimation methods for chemicals, environmental and health sciences. CRC Press, Boca Raton, FL, pp 189–231

Golet GH, Irons DB (1999) Raising young reduces body condition and fat stores in black-legged kittiwakes. Oecologia 120:530–538

Golet GH, Irons DB, Costa DP (2000) Energy costs of chick rearing in Black-legged kittiwakes (Rissa tridactyla). Can J Zool 78:982–991

Gregory-Eaves I, Demers MJ, Kimpe L, Krummel EM, Macdonald RW, Finney BP, Blais JM (2007) Tracing salmon-derived nutrients and contaminants in freshwater food webs across a pronounced spawner density gradient. Environ Toxicol Chem 26:1100–1108

Hall AJ, Gulland FMD, Ylitalo GM, Greig DJ, Lowenstine L (2008) Changes in blubber contaminant concentrations in California sea lions (*Zalophus californianus*) associated with weight loss and gain during rehabilitation. Environ Sci Technol 42:4181–4187

Hamelink JL, Waybrant RC, Ball RC (1971) A proposal: exchange equilibria control the degree chlorinated hydrocarbons are biologically magnified in lentic environments. Trans Am Fish Soc 100:207–214

Hansson MC, Persson ME, Larsson P, von Schantz T (2009) Polychlorinated biphenyl (PCB) load, lipid reserves and biotransformation activity in migrating Atlantic salmon from River Mörrum, Sweden. Environ Pollut 157:3396–3403

Harkey GA, Klaine SJ (1992) Bioconcentration of trans-chlordane by the midge, *Chironomus decorus*. Chemosphere 24:1911–1919

Hario M, Hirvi J, Hollmén T, Rudbäck E (2004) Organochlorine concentrations in diseased versus healthy gull chicks from the northern Baltic. Environ Pollut 127:411–423

Henriksen EO, Gabrielsen GW, Skaare JU (1996) Levels and congener pattern of polychlorinated biphenyls in kittiwakes (*Rissa tridactyla*), in relation to mobilization of body-lipids associated with reproduction. Environ Pollut 92:27–37

Hendry AP, Berg OK (1999) Secondary sexual characters, energy use, senescence, and the cost of reproduction in sockeye salmon. Can J Zool 77:1663–1675

Hickie BE, Mackay D, de Koning J (1999) A lifetime pharmacokinetic model for hydrophobic contaminants in marine mammals. Environ Toxicol Chem 18:2622–2633

Hickie BE, Kingsley MCS, Hodson PV, Muir DCG, Beland P, Mackay D (2000) A modelling-based perspective on the past, present, and future polychlorinated biphenyl contamination of the St. Lawrence beluga whale (*Delphinapterus leucas*) population. Can J Fish Aquat Sci 57(suppl 1):101–112

Hickie BE, Addison R, Muir DCG (2005) Development and application of bioaccumulation models to assess persistent organic pollutant temporal trends in arctic ringed seal (*Phoca hispida*) populations. Sci Total Environ 351–352:417–430

Hickie BE, Ross PS, Macdonald RW, Ford JK (2007) Killer whales (*Orcinus orca*) face protracted health risks associated with lifetime exposure to PCBs. Environ Sci Technol 41:6613–6619

Hock RJ (1960) Seasonal variation and physiologic functions of Arctic ground squirrels and black bears. Comp Zool Bull 124:155–171

Humphries MM, Umbanhowar J, McCann KS (2004) Bioenergetic prediction of climate change impacts on northern mammals. Integr Comp Biol 44:152–162

Jackson ZJ, Quist MC, Larsheid LG (2008) Growth standards for nine North American fish species. Fisheries Manag Ecol 15:107–118

Jandacek RJ, Anderson N, Liu M, Zheng S, Yang Q, Tso P (2005) Effects of yo-yo diet, caloric restriction, and olestra on tissue distribution of hexachlorobenzene. Am J Physiol Gastrointest Liver Physiol 288:292–299

Jobling M, Johansen SJS, Foshaug H, Burkow IC, Jorgensen EH (1998) Lipid dynamics in anadromous Arctic charr, *Salvelinus alpinus* (L.): seasonal variations in lipid storage depots and lipid class composition. Fish Physiol Biochem 18:225–240

Jørgensen EH, Bye BE, Jobling M (1999) Influence of nutritional status on biomarker responses to PCB in the arctic charr (Salvelinus alpinus). Aquat Toxicol 44:233–244

Jørgensen EH, Foshaug H, Andersson P, Burkow IC, Jobling M (2002) Polychlorinated biphenyl toxicokinetics and P4501A responses in anadromous Arctic charr during winter emaciation. Environ Toxicol Chem 21:1745–1752

Kaitaranta JK, Ackman RG (1981) Total lipids and lipid classes of fish roe. Comp Biochem Physiol Part B Biochem Mol Biol 69:725–729

Kannan K, Hun Yun S, Rudd RJ, Behr M (2010) High concentrations of persistent organic pollutants including PCBs, DDT, PBDEs and PFOS in little brown bats with white-nose syndrome in New York, USA. Chemosphere 80:613–618

Kawahara A, Baker BS, Tata JR (1991) Developmental and regional expression of thyroid-hormone receptor genes during *Xenopus* development. Development 112:933–943

Kelly BC, Gobas FAPC (2001) Bioaccumulation of persistent organic pollutants in lichen–caribou–wolf food chains of Canada's central and western Arctic. Environ Sci Technol 35:325–334

Kelly BC, Gobas FAPC (2003) An Arctic terrestrial food chain bioaccumulation model for persistent organic pollutants. Environ Sci Technol 37:2966–2974

Kelly BC, Gobas FAPC, McLachlan MS (2004) Intestinal absorption and biomagnification of organic contaminants in fish, wildlife and humans. Environ Toxicol Chem 23:2324–2336

Kelly BC, Ikonomou MG, Blair JD, Morin AE, Gobas FAPC (2007a) Food web-specific biomagnification of persistent organic pollutants. Science 317:236–239

Kelly BC, Gray SL, Ikonomou MG, Macdonald JS, Bandiera SM, Hrycay EG (2007b) Lipid reserve dynamics and magnification of persistent organic pollutants in spawning sockeye salmon (Oncorhynchus nerka) from the Fraser River, British Columbia. Environ Sci Technol 41:3083–3089

Kelly BC, Ikonomou MG, MacPherson N, Sampson T, Patterson DA, Dubetz C (2011) Tissue residue concentrations of organohalogens and trace elements in adult Pacific salmon returning to the Fraser River, British Columbia, Canada. Environ Toxicol Chem 30:367–376

Kirk KL (1997) Life-history responses to variable environments: starvation and reproduction in planktonic rotifers. Ecology 78:434–441

Kitchell JF, Stewart DJ, Weininger D (1977) Application of a bioenergetics model to yellow perch (*Perca flavescens*) and walleye (*Stizostedion vitreum vitreum*). J Fish Res Bd Can 34:1922–1935

Klaassen M (1996) Metabolic constraints on long-distance migration in birds. J Exp Biol 199:57–64

Kleinow K, Baker J, Nichlos J, Gobas F, Parkerton T, Muir DCG, Monteverdi G, Mastrodone P (1999) Exposure, uptake and disposition of chemicals in reproductive and developmental stages of selected oviparous vertebrates. In: Di Giulo RT, Tillittt DE (eds) Reproductive and developmental effects of contaminants in oviparous vertebrates. Society of Environmental Toxicology and Chemistry, Pensacola, FL, USA, pp 9–111

Knott KK, Schenk P, Beyerlein S, Boyd D, Ylitalo G, O'Hara TO (2011) Blood based biomarkers of selenium and thyroid status indicates possible adverse biological effects of mercury and polychlorinated biphenyls in Southern Beaufort Sea polar bears. Environ Res 111:1124–1136

Krummel EM, Macdonald RW, Kimpe LE, Gregory-Eaves I, Demers MJ, Smol JP, Finney B, Blais JM (2003) Aquatic ecology: delivery of pollutants by spawning salmon. Nature 425:255–256

Lambert Y, Dutil JD (2000) Energetic consequences of reproduction in Atlantic cod (*Gadus morhua*) in relation to spawning level of somatic energy reserves. Can J Fish Aquat Sci 57:815–825

Landrum PF, Tigue EA, Kane Driscoll SB, Gossiaux DC, Van Hoof PL, Gedeon ML, Adler M (2001) Bioaccumulation of PCB congeners by *Diporeia spp*. kinetics and factors affecting bioavailability. J Great Lakes Res 27:117–133

Larsson P (1984) Transport of PCBs from aquatic to terrestrial environments by emerging chironomids. Environ Poll 34:283–289

Leblanc GA (1995) Trophic-level differences in bioconcentration of chemicals: implications in assessing environmental biomagnification. Environ Sci Technol 29:154–160
Leney J, Drouillard KG, Haffner DG (2006a) Does metamorphosis increase the susceptibility of frogs to highly hydrophobic contaminants? Environ Sci Technol 40:1491–1496
Leney JL, Balkwill KC, Drouillard KG, Haffner GD (2006b) Determination of polychlorinated biphenyl and polycyclic aromatic hydrocarbon elimination rates in adult green and leopard frogs. Environ Toxicol Chem 25:1627–1634
Lohmann R, MacFarlane JK, Gschwend PM (2005) Importance of black carbon to sorption of native PAHs, PCBs, and PCDDs in Boston and New York Harbor sediments. Environ Sci Technol 39:141–148
Lydersen C, Wolkers H, Severinsen T, Kleivane L, Nordøy ES, Skaare JU (2002) Blood is a poor substrate for monitoring pollution burdens in phocid seals. Sci Total Environ 292:193–203
Lyman CP, Willis SJ, Malan A, Wang LCH (1982) Hibernation and torpor in mammals and birds. Academic, New York, NY
MacDonald R, Mackay D, Hickie B (2002) Contaminant amplification in the environment. Environ Sci Technol 36:456–462
Mackay D (1979) Finding fugacity feasible. Environ Sci Technol 13:1218–1223
Mackay D, Paterson S (1981) Calculating fugacity. Environ Sci Technol 15:1006–1014
Mackay D (1982) Correlation of bioconcentration factors. Environ Sci Technol 16:274–278
Mackay D (1991) Multimedia environmental models: the fugacity approach. Lewis Publishers, Chelsea, MI, pp 1–257
Mackay D, Fraser A (2000) Bioaccumulation of persistent organic chemicals: mechanisms and models. Environ Pollut 110:375–391
McCarty LS, Landrum PF, Luoma SN, Merten AA, Shephard BK, van Wezel AP (2011) A review of tissue residues in environmental toxicology. Integr Environ Assess Manag 7:7–27
McElroy AE, Barron MG, Beckvar N, Driscoll SBK, Meador JP, Parkerton TF, Preuss TG, Steevens JA (2011) A review of the tissue residue approach for organic and organometallic compounds in aquatic organisms. Integr Environ Assess Manag 7:50–74
McLachlan MS (1996) Bioaccumulation of hydrophobic chemicals in agricultural food chains. Environ Sci Technol 30:252–259
McNab BK (2001) The physiological ecology of vertebrates: a view from energetics. Cornell University Press, Cornell
McWilliams SR, Guglielmo C, Pierce B, Klaassen M (2004) Flying, fasting, and feeding in birds during migration: a nutritional and physiological ecology perspective. J Avian Biol 35:377–393
Meylen WM, Howard PH, Boethling DA, Printup H, Gouchie S (1999) Improved method for estimating bioconcetration/bioaccumulation factor from octanol/water partition coefficient. Environ Toxicol Chem 18:664–672
Montie EW, Fair PA, Bossart GD, Mitchum GB, Houde M, Muir DCG, Letcher RJ, McFee WE, Starczak VR, Stegeman JJ, Hahn ME (2008) Cytochrome P4501A1 expression, polychlorinated biphenyls and hydroxylated metabolites, and adipocyte size of bottlenose dolphins from the Southeast United States. Aquat Toxicol 86:397–412
Morrison HA, Gobas FAPC, Lazar R, Whittle DM, Haffner GD (1997) Development and verification of a benthic/pelagic food web bioaccumulation model for PCB congeners in western Lake Erie. Environ Sci Technol 31:3267–3273
Muir DCG, De Wit CA (2010) Trends of legacy and new persistent organic pollutants in the circumpolar Arctic: overview, conclusions, and recommendations. Sci Total Environ 40:3044–3051
Nakata H, Kanaan K, Jing L, Thomas NJ, Tanabe S, Giesy JP (1998) Accumulation pattern of organochlorine pesticides and polychlorinated biphenyls in southern sea otters (*Enhydra lutris nereis*) found stranded along coastal California, USA. Environ Pollut 103:45–53
Neely W, Branson D, Blau G (1974) Partition coefficient to measure bioconcentration potential of organic chemicals in fish. Environ Sci Technol 8:1113–1115

Nelson RA (1978) Urea metabolism in the hibernating black bear. Kidney Int 13:S177–S179
Nelson RA, Folk GE Jr, Pfeiffer EW, Craighead JJ, Jonkel CJ, Steiger DL (1983) Behavior, biochemistry, and hibernation in black, grizzly, and polar bears. Intl Conf Bear Res Manage 5:284–290
Ng CA, Gray KA (2009) Tracking bioaccumulation in aquatic organisms: a dynamic model integrating life history characteristics and environmental change. Ecol Model 220:1266–1273
Nichols JW, Bonnell M, Dimitrov SD, Escher BI, Han X, Kramer NI (2009) Bioaccumulation assessment using predictive approaches. Int Environ Assess Manage 5:577–597
Nilssen KT, Haug T, Potelov V, Stasenkov VA, Timoshenko YK (1995) Food habits of harp seals (*Phoca groenlandica*) during lactation and moult in March–May in the southern Barents Sea and White Sea. ICES J Mar Sci 52:33–41
Norstrom RJ, Clark TP, Jeffrey DA, Won HT, Gilman AP (1986a) Dynamics of organochlorine compounds in herring gulls (*Larus argentatus*): I. Distribution and clearance of [14C]DDE in free-living herring gulls. Enviro Toxicol Chem 5:41–48
Norstrom RJ, Clark TP, Kearney JP, Gilman AP (1986b) Herring gull energy requirements and body constituents in the Great Lakes. Ardea 74:1–23
Norstrom RJ, Clark TP, Enright M, Leung B, Drouillard KG, MacDonald CR (2007) ABAM, a model for bioaccumulation of POPs in birds: validation for adult herring gulls and their eggs in lake Ontario. Environ Sci Technol 41:4339–4347
Olivereau M, Olivereau JM (1997) Long-term starvation in the European eel: effects and responses of pituitary growth hormone-GH and somatolactin-SL secreting cells. Fish Physiol Biochem 17:261–269
Oliver BG, Niimi AJ (1988) Trophodynamic analysis of polychlorinated biphenyl congeners and other chlorinated hydrocarbons in the Lake Ontario ecosystem. Environ Sci Technol 22:388–397
Orlofske SA, Hopkins WA (2009) Energetics of metamorphic climax in the pickerel frog (*Lithobates palustris*). Comp Biochem Physiol A Mol Integr Physiol 154:191–196
Ohmiya Y, Nakai K (1977) Effect of starvation on excretion distribution and metabolism of DDT in mice. Tobuku J Exp Med 122:143–153
Paterson G, Drouillard KG, Haffner GD (2007a) PCB elimination by yellow perch (*Perca flavescens*) during an annual temperature cycle. Environ Sci Technol 41:824–829
Paterson G, Drouillard KG, Leadley TA, Haffner GD (2007b) Long-term PCB elimination by three sizes classes of yellow perch (*Perca flavescens*). Can J Fish Aquat Sci 64:1222–1233
Pelletier C, Doucet E, Imbeault P, Tremblay A (2002) Associations between weight loss-induced changes in plasma organochlorine concentrations, serum T3 concentration, and resting metabolic rate. Toxicol Sci 67:46–51
Perkins CR, Barclay JS (1997) Accumulation and mobilization of organochlorine contaminants in wintering greater scaup. J Wildl Man 61:444–449
Piersma T (2002) Energetic bottlenecks and other design constraints in avian annual cycles. Integr Comp Biol 42:51–67
Polischuk SC, Letcher RJ, Norstrom RJ, Ramsay MA (1995) Preliminary results on the kinetics of organochlorines in western Hudson Bay polar bear (Ursus maritimus). Sci Total Environ 160(161):465–472
Polischuk SC, Norstrom RJ, Ramsay MA (2002) Body burdens and tissue concentrations of organochlorines in polar bears (*Ursus maritimus*) vary during seasonal fasts. Environ Pollut 118:29–39
Post JR, McQueen DJ (1988) Ontogenetic changes in the distribution of larval and juvenile yellow perch (*Perca flavescens*): a response to prey or predators? Can J Fish Aquat Sci 45:1820–1826
Potter L, Kidd D, Standiford D (1975) Mercury levels in Lake Powell. Bioamplification of mercury in man-made desert reservoir. Environ Sci Technol 9:41–46
Quabius ES, Nolan DT, Allin CJ, Wendelaar Bonga SE (2000) Influence of dietary exposure to polychlorinated biphenyl 126 and nutritional state on stress response in tilapia (Oreochromis mossambicus) and rainbow trout (Oncorhynchus mykiss). Environ Toxicol Chem 19: 2892–2899

Ramsay MA, Nelson RA, Stirling I (1991) Seasonal changes in the ratio of serum urea to creatinine in feeding and fasting polar bears. Can J Zool 69:298–302

Randall RC, Young DR, Lee H II, Echols SF (1998) Lipid methodology and pollutant normalization relationships for neutral nonpolar organic pollutants. Environ Toxicol Chem 17:788–791

Rasmussen JB, Rowan DJ, Lean DRS, Carey JH (1990) Food chain structure in Ontario lakes determines PCB levels in lake trout (*Salvelinus namaycush*) and other pelagic fish. Can J Fish Aquat Sci 47:2030–2038

Richman LA, Hobson G, Williams DJ, Reiner E (2011) The Niagara River mussel biomonitoring program (*Elliptio complanata*): 1983–2009. J Great Lakes Res 37:213–225

Roose P, Cooreman K, Vyncke W (1998) PCBS in cod (*Gadus morhua*), flounder (*Platichthys flesus*), blue mussel (*Mytilus edulis*) and brown shrimp (*Crangon crangon*) from the belgian continental shelf: relation to biological parameters and trend analysis. Chemosphere 37:2199–2210

Russell R, Gobas FAPC, Haffner GD (1999a) Role of chemical and ecological factors in trophic transfer of organic chemicals in aquatic food webs. Environ Toxicol Chem 18:1250–1257

Russell R, Gobas FAPC, Haffner GD (1999b) Maternal transfer and in-ovo exposure of organochlorines in oviparous organisms: a model and field verification. Environ Sci Technol 33:416–420

Safe SH (1994) Polychlorinated biphenyls (PCBs): environmental impact, biochemical and toxic responses, and implications for risk assessment. Crit Rev Toxicol 24:87–149

Schlummer M, Moser GA, McLachlan MS (1998) Digestive tract absorption of PCDD/Fs, PCBs, and HCB in humans: mass balances and mechanistic considerations. Toxicol Appl Pharm 152:128–137

Schneider JE (2004) Energy balance and reproduction. Physiol Behav 81:289–317

Schulz R, Dabrowski JM (2001) Combined effects of predatory fish and sublethal pesticide contamination on the behavior and mortality of mayfly nymphs. Environ Toxicol Chem 20:2537–2543

Schwarzenbach RP, Gschwend PM, Imboden DM (1993) Environmental organic chemistry. Wiley, Toronto, ON, Canada, 681 pp

Scott WB, Crossman EJ (1973) Freshwater fishes of Canada. Fish Res Board Can, Ottawa, pp 1–966

Scott WB, Crossman EJ (1998) Freshwater fishes of Canada. Galt House Pub, Oakville, Canada

Selck H, Drouillard K, Eisenreich K, Koelmans AA, Palmqvist A, Ruus A, Salvito D, Schultz I, Stewart R, Weisbrod A, van den Brink NW, van den Heuvel-Greve M (2012) Explaining differences between bioaccumulation measurements in laboratory and field data through use of a probabilistic modeling approach. Integr Environ Assess Manag 8:42–63

Sijm DTHM, Seinen W, Opperhulzen A (1992) Life-cycle biomagnification study in fish. Environ Sci Technol 26:2162–2174

Sodergren A, Ulfstrand S (1972) DDT and PCB relocate when caged robins use fat reserves. Ambio 1:36–40

Sonne C, Wolkers H, Rigét FF, Jensen JB, Teilmann J, Jenssen BM, Fuglei E, Ahlstrøm Ø, Dietz R, Muir DC, Jørgensen EH (2009) Mineral density and biomechanical properties of bone tissue from male Arctic foxes (*Vulpes lagopus*) exposed to organochlorine contaminants and emaciation. Comp Biochem Phys C 149:97–103

Sørmo EG, Skaare JU, Lydersen C, Kovacs KM, Hammill MO, Jenssen BM (2003) Partitioning of persistent organic pollutants in grey seal (*Halichoerus grypus*) mother-pup pairs. Sci Total Environ 302:145–155

Stickel L, Stickel W (1969) Distribution of DDT residues in tissues of birds in relation to mortality, body condition, and time. Ind Med 38:44–53

Stickel WH, Stickel LF, Dyrland RA, Hughes DL (1984) Aroclor 1254 residues in birds: lethal levels and loss rates. Arch Environ Contam Toxicol 13:7–13

Subramanian AN, Tanabe S, Hidaka H, Tatsukawa R (1986) Bioaccumulation of organochlorines (PCBs and p, p,-DDE) in Antarctic Adelie penguins Pygoscelis adeliae collected during a breeding season. Environ Pollut 40:173–189

Svihla S, Bowman HC (1954) Hibernation in the American black bear. Am Midland Nat 52:248–252

Thomann RV (1981) Equilibrium model of fate of microcontaminants in diverse aquatic food chains. Can J Fish Aquat Sci 38:280–296

Thomann RV, Connolly JP, Parkerton TF (1992) An equilibrium model of organic chemical accumulation in aquatic food webs with sediment interaction. Environ Toxicol Chem 11:615–629

Tremblay A, Pelletier C, Doucet E, Imbeault P (2004) Thermogenesis and weight loss in obese individuals: a primary association with organochlorine pollution. Int J Obes 28:936–939

Van Ginneken V, Palstra A, Leonards P, Nieveen M, Berg H, Flik G, Spannings T, Niemantsverdriet P, Thillart G, Murk T (2009) PCBs and the energy costs of migration in European silver eel (*Anguilla anguilla*). Aquat Toxicol 92:213–220

Van Velzen AC, Stiles WB, Stickel LF (1972) Lethal mobilization of DDT by cowbirds. J Wildl Manage 36:733–739

Veith GD, DeFoe DL, Bergstedt BC (1979) Measuring and estimating the bioconcentration factor of chemicals in fish. J Fish Res Board Can 36:1040–1048

Walford RL, Mock D, MacCallum T, Laseter JL (1999) Physiologic changes in humans subjected to severe, selective calorie restriction for two years in biosphere 2: health, aging, and toxicological perspectives. Toxicol Sci 52:61–65

Walker C (1990) Persistent pollutants in fish-eating sea birds—bioaccumulation, metabolism and effects. Aquatic Toxicol 17:293–324

Wang-Andersen G, Skaare JU, Prestrud P, Steinnes E (1993) Levels and congener pattern of PCBs in Arctic fox, *Alopex lagopus*, in Svalbard. Environ Pollut 82:269–275

Wang T, Hung CCY, Randall DJ (2006) The comparative physiology of food deprivation: from feast to famine. Annu Rev Physiol 68:223–251

Webster JS, Hartman KJ (2007) Possible seasonal population bottlenecks in brook trout (*Salvelinus fontinalis*) in central Appalachian headwater streams. J Freshwat Biol 22:177–187

Weis JS, Weis P (1987) Pollutants as development toxicants in aquatic organisms. Environ Health Perspct 71:77–85

Wiegand MD (1996) Composition, accumulation and utilization of yolk lipids in teleost fish. Rev Fish Biol Fish 6:259–286

Yahner RH (2012) Winter strategies. In: Wildlife behaviour and conservation. Springer, New York, pp 139–143

Yordy JE, Wells RS, Balmer BC, Schwacke LH, Rowles TK, Kucklick JR (2010) Life history as a source of variation for persistent organic pollutants (POP) patterns in a community of common bottlenose dolphins (*Tursiops truncates*) resident to Sarasota Bay, FL. Sci Total Environ 408:2163–2172

Zhao RB, Sun DY, Fu S, Wang XF, Zhao RS (2007) Bioconcentration kinetics of PCBs in various parts of the lifecycle of the tadpole *Xenopus laevis*. J Environ Sci 19:374–384